Theoretical Studies on Hydroxamic Acids

Rita Kakkar

Abstract Hydroxamic acids find many applications in chemistry and biology and have been the subject of many experimental investigations. Theoretical studies are not as frequent. However, the smallest homolog, formohydroxamic acid (FHA), has been studied at various levels, including high-level ab initio and density functional with large basis sets. All studies indicate that it exists as the Z-amide tautomer and deprotonation occurs from the nitrogen. Many combined experimental and theoretical studies confirm these conclusions. The interaction of formohydroxamic acid with solvent molecules and its adducts with various compounds have also been theoretically investigated. The higher homologs have not been studied as much. Acetohydroxamic acid, also known as Lithostat, has also been investigated at various levels of theory and experiment. Interest in this compound arises from the fact that it is a known inhibitor of urease. Other investigated hydroxamic acids include benzohydroxamic acid, whose conformational properties have also been investigated. Because of their association with inhibition of the urease enzyme and matrix metalloproteinases, as well as their application as siderophores, the complexation chemistry of hydroxamic acids is very important. However, very few theoretical studies aimed at deciphering the complexation of hydroxamic acids have appeared in the literature. Studies on metal ion selectivity of hydroxamic acids reveal that the affinity toward Ni(II), the metal ion present in urease, is due to its electrophilic nature. However, several QSAR and docking studies have appeared in the literature relating to applications of hydroxamic acids as inhibitors.

Keywords DFT · Conformation · Tautomerism · Metal ion selectivity · Complexation · Urease inhibition

R. Kakkar (✉)
Department of Chemistry, University of Delhi, Delhi 110007, India
e-mail: rkakkar@chemistry.du.ac.in

S. P. Gupta (ed.), *Hydroxamic Acids*, DOI: 10.1007/978-3-642-38111-9_2,

Abbreviations

AHA	Acetohydroxamic acid
AIMD	Ab initio molecular dynamics
BHA	Benzohydroxamic acid
BPU	*Bacillus pasteurii*
DFT	Density functional theory
FHA	Formohydroxamic acid
GGA	Generalized gradient approximation
HDAC	Histone deacetylase
HOMO	Highest occupied molecular orbital
HP	*Helicobacter pylori*
HSAB	Hard and soft (Lewis) acids and bases
IW	Irving-Williams
KAU	*Klebsiella aerogenes*
KCX	Lysine NZ-carboxylic acid
LDA	Local density approximation
LUMO	Lowest unoccupied molecular orbital
MD	Molecular dynamics
MMP	Matrix metalloproteinase
NBPT	N-(n-Butyl) thiophosphoric triamide
OXHA	Oxalodihydroxamic acid
PBE	Perdew-Burke-Ernzerhof
PDF	Peptide deformylase
QSAR	Quantitative structure activity relationships
SHA	Salicylhydroxamic acid

Contents

1 Introduction

According to the IUPAC Gold Book (McNaught and Wilkinson 1997), hydroxamic acids are "Compounds, RC(=O)NHOH, derived from oxoacids $R_kE(=O)_l(OH)_m$ ($l \neq 0$) by replacing –OH by –NHOH, and hydrocarbyl derivatives thereof. Specific examples are preferably named as *N*-hydroxy amides". They contain the oxime (–N–OH) and the carbonyl (C=O) groups and have the following structure:

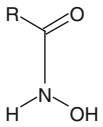

Hydroxamic acids are hydrophilic organic compounds that can exhibit keto-iminol tautomerism, and both tautomers may exist as **Z** (*zusammen*) or **E** (*entgegen*) diastereomers. They are much weaker acids than the structurally related carboxylic acids RC(=O)OH, and produce hydroxamate ions. The deprotonation could be either from the nitrogen or the oxygen, making them N-acids or O-acids. The hydroxamic acid grouping imparts chelating properties to these acids and their *N*-substituted derivatives, which serve as bidentate di-oxygen ligands toward many metal ions such as Fe(III) and Cu(II). The complexes are highly colored and are useful for the spectrophotometric (Agrawal and Patel 1980) and gravimetric (Agrawal and Roshania 1980) analysis of the metal ions.

Hydroxamate ions are best known as iron chelators (Miller 1989). Some hydroxamates are siderophores, which are compounds produced by microorganisms for the abstraction of iron from iron-deficient environments (Kehl 1982; Raymond et al. 1984; Weinberg 1989). Hydroxamate siderophores have been studied extensively due to their role as Fe(III)-specific sequestering agents, and potential pharmacological applications connected either with the microbial Fe(III) transport role or with the in vivo decontamination of Fe(III)-overload patients. Though the relationship between the biological effects and the strong chelating ability of hydroxamic acids is well established, very little is known about the metal complexes formed with natural cyclic monohydroxamic acids (Hiriart et al. 1985; Tipton and Buell 1970). This is due to the decomposition of these compounds in solution and precipitation in the presence of metal ions such as Cu(II).

Hydroxamic acids have particular affinities for 'hard' cations such as Fe(III), Np(IV), and Pu(IV) (Baroncelli and Grossi 1965; Barocas et al. 1966; Desaraju and Winston 1986; Taylor et al. 1998) with which they form five-membered chelate rings. The strong complexation of hydroxamic acids with plutonium has been used for the elimination of actinides and other hazardous metal ions from radioactive wastewater streams and for the recovery of plutonium and its extraction. They can also reduce a range of metal ions, such as Np(VI), which is very rapidly reduced to Np(V) (Colston et al. 2000).

On acid hydrolysis of free hydroxamic acids, hydroxylamine and the parent carboxylic acid are formed (Ghosh 1997). Metal ions bound to hydroxamates also hydrolyze, and complexes of Pu(IV) with formohydroxamic and acetohydroxamic acids (AHA) are slowly reduced to free Pu(III) ions (Todd and Wigelund 2006).

The chelating ability of hydroxamic acids has been used to link pharmaceutically useful ions such as radioactive or paramagnetic ions to monoclonal antibodies that direct the ion to a desired target tissue for tumor or tissue imaging or therapy purposes.

The use of hydroxamate coordination polymers as molecular magnets (Kahn 2000) has also been explored (Milios et al. 2002). Due to all these applications, the coordination chemistry of hydroxamates has evoked much interest (Brown et al. 2001; Gaynor et al. 2001; Marmion et al. 2004).

A variety of hydroxamic acid derivatives have recently been touted for their potential use as inhibitors of hypertension, tumor growth, inflammation, infectious agents, asthma, arthritis, and more. Other biological applications include inhibition of enzymes such as prostaglandin H synthase, peroxidases, ureases, and matrix metalloproteinases (MMPs) which degrade the barriers holding cells in place and are involved in tumor growth. Investigations of DNA cleavage by hydroxamic acids in the presence of metal ions (Chittari et al. 1998; Hashimoto and Nakamura 1995, 1996; Hashimoto et al. 1992, 1966, 1997, 1998; Joshi and Ganesh 1992, 1994a, b) have yielded promising results.

A recent theoretical study has been carried out on a new application of hydroxamic acids, as collectors for selective flotation of diaspore over aluminosilicates. Jiang et al. (2012) carried out a Density Functional Theory (DFT) study of the effect of carboxyl hydroxamic acids on the flotation behavior of diaspore and aluminosilicate minerals. Gece and Bilgiç (2010) studied the corrosion inhibition characteristics of two hydroxamic acids, i.e. oxalyldihydroxamic acid and pimeloyl-1,5-di-hydroxamic acid, on carbon steel using DFT. The authors related the inhibition efficiency to quantum chemical parameters such as E_{HOMO}, E_{LUMO}, calculated using B3LYP/6-31+G**, in order to elucidate the inhibition mechanism of these compounds. They found the inhibition to be due to the **E** isomer.

However, in spite of their various applications, very little was known about their structures for more than even 100 years after they were first reported by Lossen (1869). In the absence of spectral data, it was difficult to assign the correct structure from the various possible isomeric and tautomeric structures, and rotamers thereof in solution (Brown et al. 1982, 1991, 1996) and no experimental gas phase data concerning their structures were available. Added to that is the fact

that the various structures are close in energy, and accurate computational methods were not available at that time to distinguish between the structures. It could also not be established whether they are O-acids or N-acids, i.e., whether deprotonation takes place from –OH or –NH.

However, the correct assignment of their structures is extremely important because most of the applications of hydroxamic acids arise from their chelating ability, for which the correct orientation of the chelating atoms is essential. Theoretical methods can help provide information about the ground state conformation, and, if it is not the right conformation for chelation, the energy required to attain the required conformation.

It is no surprise, therefore, that a number of experimental and theoretical studies directed toward the elucidation of the structures and properties of hydroxamic acids have appeared in the literature. This article reviews the present-day knowledge of simple hydroxamic acids and their properties obtained from theoretical studies. The article is organized as follows: the simplest hydroxamic acid, formohydroxamic acid (FHA) has been the subject of various theoretical studies, ranging from semiempirical to ab initio and density functional. The former were found to be inaccurate for predicting the relative energies of tautomers, and so the literature concerning this acid from ab initio and density functional studies is first reviewed. This is followed by a description of the higher analogs and some simple aromatic acids. Literature pertaining to their complexation behavior is next reviewed, followed by theoretical studies on their biological activities.

2 Formohydroxamic Acid

The simplest hydroxamic acid, FHA, has been the subject of various experimental and theoretical investigations in the vapor and solution phases (Bagno et al. 1994; Bauer and Exner 1974; Blom and Günthard 1981; Bordwell et al. 1990; Bracher and Small 1970; Brown et al. 1991, 1996, 1998; Decouzon et al. 1990; Exner 1964; Fishbein and Carbone 1965; Fitzpatrick and Mageswaran 1989; García et al. 2000; Guo and Ho 1999; Larsen 1988; Lipczyñska-Kochany and Iwamura 1982; Mora-Diez et al. 2006; Remko and Šefčíková 2000; Remko 2002; Remko et al. 1993; Sałdyka and Mielke 2002, 2003a; Sant'Anna 2001; Turi et al. 1992; Ventura et al. 1993; Wang and Houk 1988; Wiberg and Laidig 1988; Wu and Ho 1998; Yazal and Pang 1999; Yen et al. 2000). In view of the diverse results obtained from previous calculations and experimental observations, Kakkar et al. (2003) carried out a systematic study of the structures of some primary and secondary hydroxamic acids: –RCONR′OH; R = H, CH_3, C_2H_5; R′ = CH_3 (formo-, aceto-, propano-, and *N*-methylacetohydroxamic acids). They determined the relative acidities and stable configurations and tautomers of the neutral and deprotonated hydroxamic acids, which can serve as model hydroxamic acids used in cancer drug design, since these acids contain the smallest unit C=O…NH that can bind to the DNA helix.

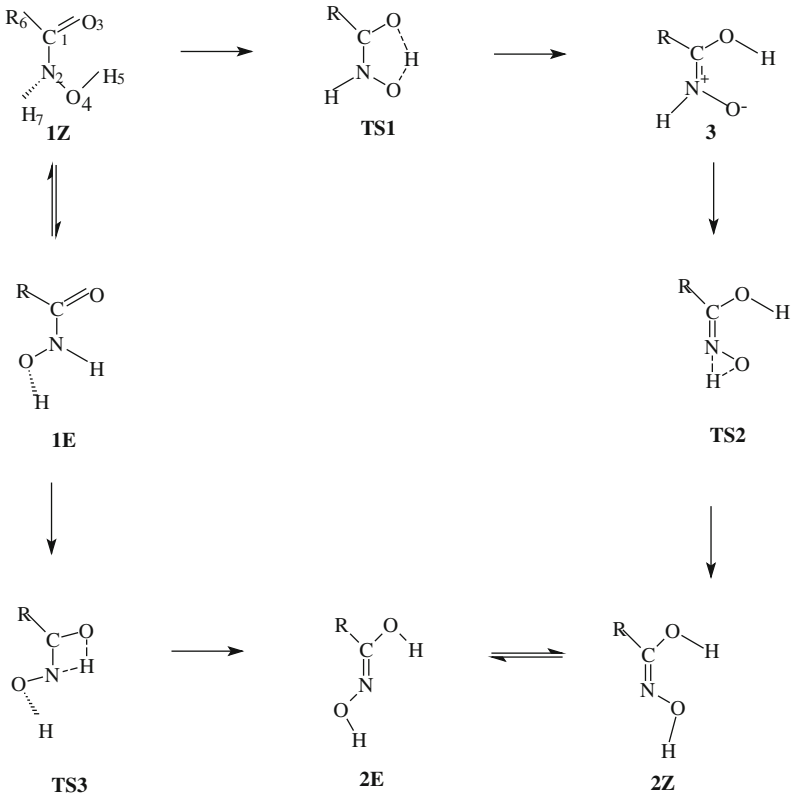

Fig. 1 The tautomeric forms of hydroxamic acids (R = H, CH_3, C_2H_5) and the transition states interconnecting them

All the systems may exist in three tautomeric forms, viz. two rotamers of the keto form (**1E**, **1Z**), two rotamers of the iminol form (**2E**, **2Z**), and one zwitterionic iminol form, **3**. The various forms and their interconversions are depicted in Fig. 1 (Wu and Ho 1998).

2.1 Relative Energies

FHA, being the smallest member of the family, has been studied at various levels of theory. Bauer and Exner (1974) reported that the keto forms, **1E** and **1Z** (Fig. 1), are favored over the iminol forms, **2E** and **2Z**. Low-level ab initio calculations suggested that the **1E** tautomer exists preferentially in the gas phase, but inclusion of correlation energy shifted the preference to **1Z** (Turi et al. 1992; Wu and Ho 1998). This conclusion was confirmed by Remko et al. (1993). The order of gas phase stability, as determined by Wu and Ho (1998) by ab initio theoretical

calculation, is **1Z** > **2Z** > **1E** > **2E**. However, experimental studies on the structure of FHA using X-ray (Larsen 1988) and ^{17}O NMR (Lipczyñska-Kochany and Iwamura 1982) indicated that the most stable structure is **1E** in its crystals and **1Z** in solution.

DFT calculations at the B3LYP/6-311++G**//B3LYP/6-31G* level (Kakkar et al. 2003) place the order of gas phase stabilities as **1Z** > **1E** > **2Z** > **2E** > **3**. Again, the keto tautomers were found to be preferred over the iminol ones, but the order of stabilities of the two rotamers of the keto form was found to be different from that reported by Wu and Ho (1998). The finding that **1Z** is more stable than **1E** agrees with the expectation based on stabilization of **1Z** due to intramolecular hydrogen bonding (see Fig. 1), and the smaller value of the dipole moment of **1Z** (3.00 D compared to 3.37 D of **1E**), which also agrees with the finding (Wang and Houk 1988; Wiberg and Laidig 1988) that the rotamer with the smaller dipole moment is always more stable in vacuum. However, the difference in energy between the **1Z** and **1E** rotamers is very small, and we may conclude that **1Z** and **1E** coexist in the gas phase, as found experimentally from IR spectra (Sałdyka and Mielke 2003a). At 298.15 K and 1 atm pressure, the Gibbs energy difference between the **1Z** and **1E** forms was found to be only 0.6 kcal mol^{-1} (Kakkar et al. 2003), which implies that **1Z** is present to the extent of ~75 %. However, none of the two semiempirical methods, AM1 and PM3, were able to give the correct order of stabilities. The two keto forms (**1Z** and **1E**) were found to be nonplanar, whereas the two iminol forms, **2E** and **2Z,** are nearly planar. Since the crystal data pertain to the **1E** form (Larsen 1988), the calculated optimized geometries for **1E** were compared with the experimental ones, and the agreement was found to be within 2 %, validating the DFT method.

These predictions were confirmed by later theoretical and experimental studies. Sałdyka and Mielke (2007) investigated the keto-iminol tautomerism of AHA and FHA isolated in argon matrixes by full Xe arc irradiation. For FHA, the relative abundances of **1Z**, **2Z**, and **1E** were found to be 94.3, 2.5, and 3.1 %, respectively, in agreement with their MP2/6-311++G(2d,2p) predicted values (85, 3.99, 11, and 0.0062 %) based on calculated ΔE_{ZPE} energies 1.43, 1.25, and 5.29 kcal mol^{-1} of **2Z**, **1E**, and **2E** relative to **1Z**.

2.2 Intramolecular Proton Transfer

The potential energy profiles for the intramolecular proton transfer of FHA tautomers (Fig. 1) have also been investigated at the G2 (Wu and Ho 1998) and DFT (Kakkar et al. 2003) levels. The energies of the transition states reflect their different respective ring strains, and the energy order is **TS2** > **TS3** > **TS1**, since the three transition states involve three, four, and five membered rings, respectively. Wu and Ho (1998) discussed in detail the transformation from the keto form (**1Z**) to the enol form (**2Z**). They concluded that, of the two possible pathways for the transformation (**2Z**, see Fig. 1), the first pathway, that is, **1Z** → **3** → **2Z**,

involves the highly strained three-centered transition state (**TS2**) and does not seem likely. The second pathway, **1Z** → **1E** → **2E** → **2Z**, involves the relatively less strained four-center-like transition state, **TS3**, and should be thus preferred. However, they did not take into account the substantial rotational barrier from **2E** to **2Z**. At the B3LYP/6-311++G**//B3LYP/6-31G* level (Kakkar et al. 2003), the barrier is 45.2 kcal mol^{-1}, which is much higher than the general rotational barrier for C–N bonds, in the range 10–15 kcal mol^{-1} (Blom and Günthard 1981). This is to be expected, since in this case the rotation is about the C=N double bond. In fact, the transition state has a higher energy (51.0 kcal mol^{-1}) than either **TS1** or **TS3**. It is therefore quite likely that the **2E** tautomer formed initially does not undergo subsequent isomerization to the more stable rotamer, **2Z**. The calculated rotational barrier separating **1Z** and **1E** is, however, much smaller (17.3 kcal mol^{-1}). The path for the transformation of **1E** to **2E** via the transition state **TS3** was found to have an activation energy of 43.4 kcal mol^{-1}, as compared with the calculated G2 (Wu and Ho 1998) barrier of 42.4 kcal mol^{-1}. Both theoretical results are in close agreement. Thus, DFT calculations, which can be performed at a fraction of the cost of the high level G2 calculations, perform as well. The overall activation energies for the two pathways are 53.5 and 51.0 kcal mol^{-1}, respectively, and the latter is only slightly preferred.

B3LYP/6-311++G* calculations on the tautomerism in some hydroxamic acids in the gas phase, in solvent, and in the presence of 1–3 water molecules (Tavakol 2009) also revealed the greater stability of the **1Z** tautomer. The calculations showed that the energy barrier of gas phase tautomerism is very high, but the presence of water molecules decreases the barrier.

Besides intramolecular hydrogen bonding that stabilizes the **1Z** tautomer, intermolecular hydrogen bonding with solvent molecules has also been theoretically investigated.

2.3 Intermolecular Hydrogen Bonding

Of the monohydrates of the **1Z** and **1E** forms of FHA, shown below, **1Z·H$_2$O** was found to be more stable than **1E·H$_2$O** by 2.5 kcal mol^{-1} (Kakkar et al. 2003). Thus, **1Z** becomes more strongly favored in aqueous solution.

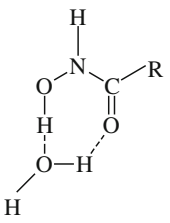

1Z.H$_2$O

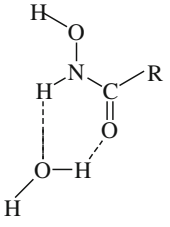

1E.H$_2$O

The reaction enthalpy for the process

$$1Z + H_2O \rightarrow 1Z \cdot H_2O$$

was found to be -8.3 kcal mol^{-1} and that for

$$1E + H_2O \rightarrow 1E \cdot H_2O$$

as -6.3 kcal mol^{-1}. Thus, hydrogen bonding with water stabilizes **1Z** to a greater extent than **1E**. Kaur and Kohli (2008) investigated the intra- and intermolecular hydrogen bonding in FHA at the MP2/6-31+G* level. They reported that intramolecular hydrogen bonding exists only in the **1Z** isomer, though there are multiple hydrogen bond donor and acceptor groups present in the other isomers. Adduct formation with a water molecule results in intermolecular hydrogen bonding, which is stronger than the intramolecular hydrogen bonding. However, their results are at variance with the experimental observation (García et al. 2003, 2005) that complexation with free hydroxamic acids is slower than that with the anions, indicating that the intramolecular hydrogen bond is hard to break, and blocks the reaction site. NMR studies have also shown lack of exchange of this proton.

Senthilkumar and Kolandaivel (2006) applied ab initio and DFT methods to study the hydrogen bonding in the complexes formed between FHA and water molecules. They found that FHA has the **1Z** form in all the complexes. ^{1}H and ^{13}C NMR, combined with B3LYP/6-311++G(d,p) chemical shifts in DMSO solution, revealed that 2-(hydroxyimino)propanohydroxamic acid forms hydrogen bonds with solvent molecules in solution (Kaczor and Proniewicz 2005), but exists as dimers in the solid state.

Sałdyka and Mielke (2005a) studied the complexes of FHA with water and ammonia using FTIR matrix isolation spectroscopy and MP2/6-311++G(2d,2p) calculations. Their analysis of the experimental spectra of the FHA/$H_2O(NH_3)$/Ar matrixes indicated formation of strongly hydrogen-bonded complexes in which the NH group of FHA acts as a proton donor toward the oxygen atom of water or the nitrogen atom of ammonia. Though theoretical calculations indicate that the most stable complexes are the cyclic structures in which the water or ammonia molecules are inserted within the intramolecular hydrogen bond of the FHA molecule and act as proton donors for the CO group and proton acceptors for the OH group of FHA, these were not observed in the matrixes, which indicates high energy barrier for their formation.

Sałdyka and Mielke (2004a, b) recorded the argon matrix infrared spectra of the complexes formed between FHA and nitrogen/carbon monoxide. In the case of nitrogen, two isomeric complexes with the nitrogen atom attached to the NH or OH group of FHA were found. Theoretical vibrational frequencies at the MP2/6-311++G(2d,2p) level were found to be in good agreement with the experimental data. Three isomeric complexes were formed with carbon monoxide: in two of the complexes, the carbon atom of carbon monoxide interacts with the NH or OH group of FHA and, in the third, the oxygen of carbon monoxide interacts with –NH

of FHA. Again, the observed vibrational frequencies were found to be in good agreement with the calculated B3LYP/6-311++G(2d,2p) values.

Kaur and Kohli (2012) investigated the hydrogen-bonding abilities of a few amino acid side chains through aggregation of methylamine, methanol, and acetic acid with formo- and thioformohydroxamic acids using MP2/6-31+G* calculations.

Denis and Ventura (2001) carried out a density functional study of the neutral and ionic chelates of boric acid with FHA. The calculated IR spectrum for the bis(hydroxamate) boron chelate was found to be in excellent agreement with the experimental spectrum.

The structures and gas phase metal affinities of FHA derivatives were studied using B3LYP/6-311+G(d,p) and CPCM solvations (Šille et al. 2010). The stability order of the alkali metal ion complexes ($Li^+ > Na^+ > K^+$) was found to be as expected on the basis of the ionic radii of the alkali metal ions.

2.4 Aqueous Phase Calculations

The calculated Gibbs energies of **1E**, **2Z**, and **2E** in aqueous solution relative to **1Z** (Kakkar et al. 2003) were found to be 7.5, 5.0, and 7.2 kcal mol^{-1} at 298.15 K and 1 atm. Thus, the **1Z** form becomes more emphatically favored in aqueous solution, in agreement with experiment (Lipczyñska-Kochany and Iwamura 1982), and the iminol forms also become apparent (stability order: **1Z** > **2Z** > **2E** > **1E**).

Aqueous solvation reduces the C–N bond length considerably, and there is a concomitant increase in the carbonyl bond length, signifying that delocalization of electrons takes place from the carbonyl bond to the carbon–nitrogen bond. The N–C and C=O stretching frequencies increase by 39 cm^{-1} and decrease by 174 cm^{-1}, respectively. The carbonyl oxygen is also involved in intermolecular hydrogen bonding with water molecules. The variation in the C–N, O–N, and O–C bond lengths in the isolated, complexed with one water molecule and in bulk water environments for the two rotamers is interesting. Solvation in **1Z** considerably reduces the C–N and O–N bond lengths, but lengthens the C–O bond only slightly. This shows that the intramolecular hydrogen bond remains intact in aqueous solution, in agreement with experimental observations (García et al. 2003, 2005). For **1E**, however, it is the C–O bond that shows the largest increase. In both cases, while the other two bonds show a constant increase or decrease in going from the isolated molecule to a complex with a single water molecule and then to bulk water, the O–N bond is shortest in the single water molecule complex, accounting for the destabilization.

2.5 Anions

Since the **1Z** form seems to be the favored one in the gas phase and in aqueous solution, dissociation could occur either from the NO–H group leading to the anion **1a**, both *cis* and *trans* forms of which are possible (Fig. 2), making FHA an

Fig. 2 Possible anion structures

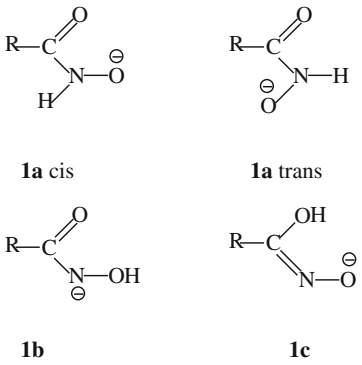

O-acid. However, if the N–H proton were to dissociate, it would be an N-acid, leading to the anion **1b**. In addition, there is a possibility of dissociation from the NO–H group of the almost equally stable **1E**, leading to structure **1c**, and making FHA an O-acid (see Fig. 2).

The **1b** anion was found (Kakkar et al. 2003) to be the most stable, followed by **1a-*cis***, **1a-*trans,*** and **1c** in that order. The finding that **1b** is more stable than the other anions agrees with other high-level ab initio (Ventura et al. 1993; Bagno et al. 1994) calculations. The greater stability of **1b** over **1a-*cis***, both of which are derived from **1Z**, can be easily explained. In the former, an electron resonance involving the N–C=O bonds is possible, which should stabilize the two unshared electron pairs on the nitrogen atom. That this occurs is confirmed by the following: The C–N bond length in **1b** reduces to 1.318 Å from 1.361 Å in **1Z**, and its vibrational frequency also increases by 56 cm^{-1}. Similarly, the carbonyl bond length increases to 1.276 Å compared to 1.225 Å in **1Z**. Its vibrational frequency also reduces by 96 cm^{-1}. This implies that a resonance exists between the keto and iminol forms, as shown below:

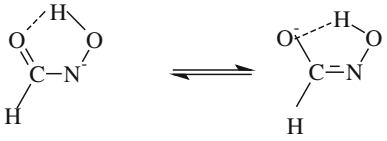

1b

keto iminol

IR studies (Exner 1964) also show a red shift in the carbonyl frequency, indicating that it is in resonance with the nitrogen lone pairs. From the calculated partial atomic charges on the various atoms in **1Z** and **1b**, it is seen that the largest increase in negative charge occurs at the carbonyl oxygen, followed by the change at the nitrogen on formation of the anion **1b** from **1Z**. This again supports the concept of resonance in the anion, as the deprotonated FHA may be considered as the nitrogen-deprotonated keto form, or, alternatively, the *C*-hydroxy oxygen-deprotonated iminol form.

In contrast, if the proton dissociates from the oxygen atom to form **1a-*cis***, no such electron resonance is possible, which can stabilize the anion, but the originally existing intramolecular hydrogen bonding also disappears, increasing the instability of the resultant anion. The greater stability of **1b** implies that FHA is an N-acid in the gas phase, and this is in accord with most experimental and theoretical conclusions (Remko et al. 1993; Wu and Ho 1998). The calculated gas phase basicity for the formohydroxate ion is 347.2 kcal mol^{-1}. However, it may be mentioned that, as the three forms **1Z**, **1E**, and **2Z** are in equilibrium in the gas phase, it may also be considered as an O-acid as a result of deprotonation from the oxygen of the **2Z** form. This is supported by the structure of the anion, which is a resonance hybrid of the two forms.

Wu and Ho (1998) also argued for N-acid behavior of hydroxamic acids thus: since structure **1Z** is the most stable conformation of FHA in the aqueous phase, its acidity would depend on which hydrogen atom (attached to the N atom or the O atom) can be dissociated easily. Since the barrier to the transformation **1Z** → **3** is smaller than that for the intramolecular proton transfer (**1Z** → **1E** → **2E** → **2Z**), the former reaction takes place faster and the proton on O_4 (H_5) is not available for dissociation, as it remains between the two oxygens, O_4 and O_3. The **1Z** to **2Z** transformation, which involves the transfer of the proton (H_7) attached to N_2, however, is more difficult and thus this proton is relatively easy to dissociate.

Leung (2006) applied ab initio molecular dynamics (AIMD) to study the hydration structures and electronic properties of the formohydroxamate anion in water. It was found that, in the O-deprotonated anions, the negative charge is concentrated on the oxime oxygen, while in the N-deprotonated case, it is partially delocalized between the nitrogen and the adjoining oxime oxygen atom.

Senthilnithy et al. (2006) carried out ab initio calculations on isomers of *N*-phenylbenzohydroxamic acid derivatives and their deprotonation process. They found that the acid dissociation constants obtained using CBS-QB3 gas phase energies and HF/6-31+G(d)/CPCM hydration energies closely agree with the experimental values, provided that the most stable isomer for the molecule and the anion in water are taken as the Z-isomer. Senthilnithy et al. (2008) treated the first hydration shell of the O-deprotonated and N-deprotonated anions explicitly using HF/6-31+G(d), and the rest of the solvent as a continuous dielectric using CPCM, and found that the O–H bond dissociation is favored in aqueous medium. They supported their cluster calculations with a molecular dynamics (MD) simulation. Dissanayake and Senthilnithy (2009) presented a thermodynamic cycle to calculate pK_a values of hydroxamic acids, including the gas phase N–H deprotonation of the hydroxamic acid, the solvent phase transformation of the N-ion to the O-ion and the solvation of the hydroxamic acid molecule and the O-ion in water. Kaur et al. (2009) also calculated the pK_a values for deprotonation from formo- and thioformohydroxamic acids and concluded that these are N-acids.

The photodecomposition of FHA yielding the hydrogen-bonded complexes HNCO–H_2O and NH_2OH–CO has been studied both experimentally and theoretically (Sałdyka and Mielke 2003b). B3LYP/6-311++G(2d,2p) calculations provided support for the proposed structures.

3 Higher Homologs

3.1 Aceto- and Propanohydroxamic Acids

The next two higher homologs of FHA are aceto- and propanohydroxamic acids. The former (AHA) is also known as Lithostat, a drug used to cure kidney ailments, although it has several side effects, such as hemolytic anemia, blood clotting, and headaches. Fishbein and Carbone (1965) first reported its function as an inhibitor of the enzyme urease.

A similar trend in energy is observed in the case of these two molecules (Kakkar et al. 2003), with the energy gap between the **1E** and **1Z** forms becoming smaller with each substitution, until for propanohydroxamic acid, the **1E** form becomes favored over **1Z**. X-ray crystallographic analysis of AHA revealed the stable structure to be the **1Z** form in the solid state (Bracher and Small 1970). The greater stability of the **1E** form for propanohydroxamic acid in the gas phase seems contrary to the fact that an intramolecular hydrogen bond in the **1Z** form is disabled in **1E**. However, the small differences in energy suggest that both aceto- and propanohydroxamic acids exist in the **1Z** and **1E** forms that are in equilibrium in the gas phase. This prediction is consistent with previous ab initio calculations (Yazal and Pang 1999). Mora-Diez et al. (2006) also reported the greater stability of the **1Z** form based on their MP2(FC)/AUG-cc-pVDZ level calculations.

Sałdyka and Mielke (2007) reported that the relative abundances of the **1Z**, **2Z**, and **1E** isomeric structures in the AHA/Ar matrixes, obtained by deposition of the vapor over solid AHA sample heated to 301 K, are 95.1, 3.7, and 1.2 %, respectively. The results of their calculations at the MP2/6-311++G(2d,2p) agreed with the experimentally determined order of stability of the AHA isomers.

As far as the activation barriers are concerned, for the pathway from **1Z** to **2E** involving **TS3,** the overall barriers are 43.4, 40.8, and 39.0 kcal mol^{-1}, respectively, for formo-, aceto-, and propanohydroxamic acids (Kakkar et al. 2003). The barriers decrease slightly with every methyl substitution.

Theoretical and experimental studies of the solvent effect on the protonation of AHA have been carried out (García et al. 2000; Munoz-Caro et al. 2000). Mora-Diez et al. (2006) calculated the structures of the aggregates of the neutral and anionic forms of AHA with a water molecule at the MP2(FC)/AUG-cc-pVDZ level of theory, in order to evaluate the effect of intermolecular hydrogen bond formation on the deprotonation processes of AHA. They reported that the intramolecular hydrogen bonding is preserved in the **1Z·H_2O** aggregate, as found for FHA (Kakkar et al. 2003), but the **1E·H_2O** system represents the most stable aggregate.

The observation that **1b** is the most stable form of the anion (Kakkar et al. 2003) agrees well with high-level ab initio and density functional calculations (Yazal and Pang 1999). Decouzon et al. (1990) measured gas phase acidities of AHA as well as those of its N-methyl and O-methyl derivatives, concluding that it behaves essentially as an N-acid in the gas phase, with a gas phase basicity of the

N-anion equal to 339.1 ± 2 kcal mol^{-1}. The theoretically calculated value of 337.1 kcal mol^{-1} (Kakkar et al. 2003) agrees well with this value. For propanohydroxamic acid, the calculated value is 335.3 kcal mol^{-1}. Other authors (Bordwell et al. 1990; Ventura et al. 1993; Bagno et al. 1994; Mora-Diez et al. 2006; Vrcek et al. 2008) also confirmed N-acid behavior for hydroxamic acids in gas phase and in DMSO solution. Kaczor and Proniewicz (2004) carried out DFT (6-311++G(d,p)) calculations of NMR spectra in DMSO solution for FHA and oxalodihydroxamic (OXHA) acid aggregates with two DMSO molecules via hydrogen bonding between the labile protons of the acids and the oxygens of the solvent molecules. They found excellent correlation between the calculated and observed NMR spectra. Again, the **Z** forms were found to be more stable, with OXHA existing exclusively in this form.

Ab initio molecular orbital calculations with 4-31G//4-31**G,** 6-3lG*//4-31G, and 6-31+G//4-31G basis sets were used to examine the structure, relative energy, protonation, and deprotonation of a series of seven hydroxamic acids in the gas phase (Yamin et al. 1996). The results showed that the most probable protonation site is the carbonyl oxygen atom, while deprotonation proceeds by loss of the NH hydrogen. MP2(FC)/AUG-cc-pVDZ calculations and NMR, spectrophotometric, and potentiometric measurements of the isomers of AHA and their deprotonation processes (Senent et al. 2003) gave essentially the same results: the **1Z** conformer is most stable in the gas phase and deprotonation occurs from the nitrogen in aqueous solution. García et al. (2000) carried out an experimental and theoretical study at the B3LYP/cc-pVDZ level on the solvent effect on protonation of AHA. They also found that the carbonyl is the most active site for protonation.

Sałdyka and Mielke (2005b) studied the dimerization of the keto tautomer of AHA using FTIR matrix isolation spectroscopy and B3LYP/6-31+G(d,p) calculations. Analysis of the AHA/Ar matrix spectra indicated formation of two dimers in which the intramolecular hydrogen bonds within the two interacting AHA molecules are retained.

Binary AHA…HX complexes of AHA with hydrogen halides, HX (X = F, Cl, Br) were investigated using the second order perturbation theory (Joshi and Gejji 2005). In the case of the complex with hydrogen fluoride, the latter acts as both a proton-donor to the carbonyl oxygen and as a proton-acceptor from the hydroxyl group. In the case of the chloro- and bromo-substituted derivatives, however, hydrogen-bonded interactions exist with the carbonyl oxygen and the methyl protons of AHA.

3.2 N-Methylacetohydroxamic Acid

In contrast to the situation for the above acids, in *N*-substituted derivatives, there is no possibility of the enol form as the nitrogen lacks a hydrogen atom for transfer to the carbonyl oxygen. In this case, too, it was found (Kakkar et al. 2003) that, like propanohydroxamic acid, the **1Z** form is less stable than **1E** by 0.8 kcal mol^{-1}.

However, the small difference suggests that both forms are in equilibrium in the gas phase. For the anion, it is found that the **1a-*trans*** form is more stable than **1a-*cis*** by 10.9 kcal mol^{-1}. This agrees with the prediction of previous ab initio calculations (Yazal and Pang 1999). The gas phase basicity of the anion (343.4 kcal mol^{-1}) agrees with the experimental value (Decouzon et al. 1990) of 346.9 ± 2 kcal mol^{-1}.

3.3 Arylhydroxamic Acids

Aromatic hydroxamic acids have also been extensively studied. García et al. (2005) carried out a theoretical and experimental study on the conformations, protonation sites, and metal complexation of benzohydroxamic acid (BHA). Their calculations at the RHF/cc-pVDZ level, refined by the B3LYP/AUG-cc-pVDZ method, indicated that, in the gas phase, **1Z** is the most stable structure of both neutral and deprotonated BHA. In acetone solution at −80 °C, the E/Z ratio was estimated as 3. They also experimentally observed the formation of E–E, Z–Z, and E–Z dimers, which dissociate in aqueous solution. The theoretical results showed that, as in AHA, intramolecular hydrogen bonding is strong. This agrees with the experimental observation in the dynamic ^{1}H NMR spectrum of BHA (García et al. 2005) in acetone solution (with residual water) that the coalescence temperature between the two proton singlets of the **E** isomer increases from −10 to 5 °C when the proportion of residual water of the solvent is increased by 30 %. This indicates that water hinders the interchange between the two protons of the E–NHOH group, probably due to hydrogen bond formation. The authors (García et al. 2003, 2005) also observed that the rate of complexation of Ni(II) with **1Z** hydroxamic acids is slower than that with the corresponding anions. This indicates that in aqueous solution, intramolecular hydrogen bonding is stronger than the intermolecular hydrogen bonding with water molecules, and this blocks the reaction site, slowing down the rate of complexation. Recently, the structure of BHA was investigated at the B3LYP, MP2, and MP4(SDQ) levels of theory and compared to the corresponding structures of formyl analogs (Al-Saadi 2012). All levels of theory predicted the molecule to exist predominantly in a near-planar structure adopting a *cis* conformation where the hydroxyl group eclipses the carbonyl bond.

For salicylhydroxamic acid (SHA) and *p*-hydroxybenzohydroxamic acid, García et al. (2007) found evidence for extended aggregation. B3LYP/AUG-cc-pVDZ level calculations showed that the most stable gas phase conformer is **1Z**, a structure with all three phenolate, carboxylate, and hydroxamate oxygen atoms in the *cis* position. The most stable monoanion is the N-deprotonated **1Z**.

For the three isomeric aminophenylhydroxamic acids, too, the **1Z** keto form was found to be the most stable (Kakkar et al. 2006a) in each case. Among the three isomers, 2-aminophenylhydroxamic acid was found to be the most stable, despite the two hydrogens in close proximity in the former. Hyperconjugative interactions with nitrogen and intramolecular hydrogen bonding reduce the

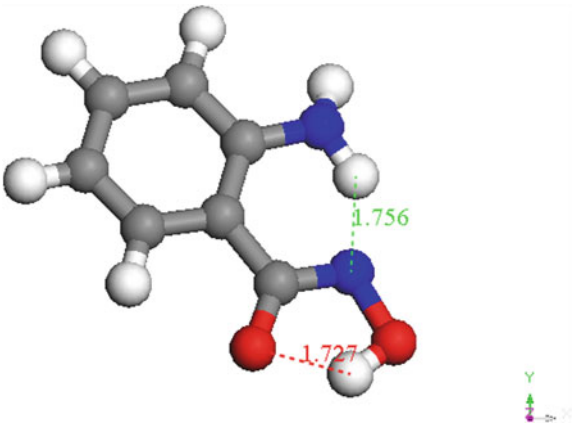

Fig. 3 Structure of the **b** anion of 2-aminophenylhydroxamic acid, showing the extensive hydrogen bonding. Distances are in Å

carbonyl bond order in the **Z** isomers of the acids. In the anions formed by deprotonation of –OH, only the hyperconjugative interactions operate, but these too reduce the carbonyl bond order to ~ 1.6.

All three acids are stabilized by intramolecular hydrogen bonding and the **Z** forms are more stable than their **E** counterparts by several kcal mol^{-1}, unlike the case of the simple hydroxamic acids. Besides, the **E** forms are nonplanar and do not represent energy minima in the case of 2-aminophenylhydroxamic acid, which possesses a small imaginary vibrational frequency (155 cm^{-1}) and the 4-aminophenyl isomer, for which the imaginary frequency is 45 cm^{-1}. In this case, too, the acids are N-acids, as the **b** anion is more stable than **a** in all cases. The difference in energies between the two anions is highest for the anion of 2-aminophenylhydroxamic acid (19.5 kcal mol^{-1}), as there is extensive hydrogen bonding in the **b** anion in this case (see Fig. 3). This partly explains why this isomer has a tendency to form complexes by deprotonation from both nitrogen and oxygen, while the other acids undergo deprotonation at oxygen only on complex formation.

4 Metal Ion Chelation

By far, the most important application of hydroxamic acids is as metal ion chelators. The coordination chemistry of hydroxamic acids has been reviewed (Codd 2008), laying emphasis on the expansive role of hydroxamic acids in chemical biology.

Metal-hydroxamate complexes exhibit structural diversity (Dessi et al. 1992; Farkas et al. 1998a, b, 2000; Gaynor et al. 2001; Kurzak et al. 1992; Marmion et al. 2000; Milios et al. 2002). Hydroxamate ions have two oxygen atoms and may bond to the metal ion in two different ways: monodentate or bidentate

configurations. Besides, they may also coordinate through the nitrogen atom and one oxygen atom. However, the bulk of experimental data favor the bidentate mode using two oxygen atoms. An X-ray diffraction study of the Fe(III) complex showed that the chelation involves the oxygen belonging to the carbonyl and NHOH groups (Lindner and Göttlicher 1969). Investigations on the complex formation with simple primary hydroxamic acid ligands in aqueous solution demonstrated clearly that, depending on the pH, two (O,O) binding modes of the ligands are accessible to metal ions like Cu(II) and V(IV) (Dessi et al. 1992; Farkas et al. 1998a). The more common hydroxamato (1-) type mode arises from the first deprotonation step and involves the coordination of the NHO^- moiety. The hydroximato (2-) form of the ligand is produced by further metal-induced deprotonation of the NHO^- at high pH. The coordination of the nitrogen atom of the hydroxamic moiety was never found in metal complexes formed by simple hydroxamic acids. Hydroxamic acids have been found to bind in other coordination modes as well (Milios et al. 2002).

However, in order to chelate to metal ions, the acid should adopt the required *cis* (**Z**) conformation. The reaction scheme shown in Fig. 1 entails rotations about the C–N bond for the interconversion between the two pairs of rotational isomers **1Z**, **1E** and **2Z**, **2E**. While the latter barrier is quite high, the smaller barrier to the CN rotation from **1Z** to **1E** plays an important role in metal ion chelation. The effects of this barrier are also reflected in kinetic parameters obtained from the sequestration of iron by hydroxamic acids from the polynuclear iron complex, $[Fe_{11}O_6(OH)_6(O_2CPh)_{15}]$. The substituents at nitrogen and carbon can modify the *cis*/*trans* (**Z**/**E**) ratio, as was found for a series of monohydroxamic acids (Brown et al. 1991, 1996). As the required conformation for the formation of a normal (O,O) chelate is *cis*, correlation between the **Z**/**E** ratio and the stability of the chelate (both thermodynamic and kinetic), can be expected.

4.1 Barriers to Rotation

For FHA, the calculated (Kakkar et al. 2003) rotational barriers at the DFT level in the gas phase and in aqueous solution are, respectively, 17.9 and 20.2 kcal mol^{-1}, respectively. For AHA, the gas phase barrier is calculated as 16.7 kcal mol^{-1}. Thus, the rotational barriers increase on aqueous solvation. Although the MP2/6-311G** calculations (Brown et al. 1998) predict otherwise, the rotational barriers decrease with increasing methyl substitution for the gas phase. Part of the discrepancy between the DFT results and those of Brown et al. (1998) could be due to underestimation of the stability of the **Z** form in their calculations, because of non-inclusion of diffuse functions that could lead to an incorrect description of hydrogen bonding effects. For *N*-methyl acetohydroxamic acid, the calculated rotational barrier from the more stable **1E** form is 16.6 kcal mol^{-1}, as compared with a value of 16.0 kcal mol^{-1} from MP2/6-311G** calculations (Brown et al.

1998). Niño et al. (2000) compared their MP2(FC)/cc-pVDZ and B3LYP/cc-pVDZ results for barriers to nitrogen inversion and methyl rotation in AHA, and found large differences in the two results.

4.2 Choice of an Appropriate Methodology

Hydroxamic acids are known to inhibit urease, a nickel-containing metalloenzyme. Three factors determine the specificity of a given metal-binding site for a particular transition metal ion (Bertini et al. 1995; Rulísék and Vondrášek 1998): the coordination geometry, the size of the preformed cavity in more complex ligands, and the affinity of functional groups participating in metal–ligand bonds for a specific transition metal ion. The third factor, and probably the most difficult one to address, is the different affinities of a particular ligand for different transition metal ions, which is often based on qualitative or semi-quantitative theories or principles such as the hard and soft acids and bases (HSAB) principle of Parr and Pearson (1983) and Pearson (1963) and the Irving-Williams (IW) series of stability constants (Sigel and McCormick 1970; Martin 1987). Nevertheless, a quantitative evaluation of the affinity is feasible only with accurate quantum chemical calculations on model systems, which is why a reliable computational scheme for the calculation of transition metal complexes containing metal–ligand bonds with ionic character is desired.

However, due to several reasons, there are very few quantum mechanical calculations on the electronic effects in the interaction of metal ions with biological systems. The first reason is the large number of electrons and spin states that must be considered for transition metal ions owing to their partially filled *d* orbitals, which makes it difficult to assign the ground spin state. Unrestricted calculations, which take up twice as much time as the restricted calculations, need to be performed on these systems in order to identify the ground state. Often the basis sets for these metal ions are also unavailable. The SCF convergence is also slow, owing to the mixing of the *d* orbitals with the *s* orbitals. Moreover, Jahn-Teller distortions remove symmetries, making the calculations even more computationally expensive. Nevertheless, advances in computational methodologies have now made it possible to perform accurate DFT calculations at modest cost and with reasonable accuracy, which sometimes even surpasses experimental determinations. In particular, Generalized Gradient Approximation (GGA) combines accuracy with reasonable computational cost.

Hydroxamic acids, particularly AHA, are known inhibitors of the urease enzyme. They block the Ni(II) ion of the enzyme by binding selectivity to it. The particular affinity of hydroxamic acids for Ni(II) was investigated (Kakkar et al. 2006b). In this study, the authors compared the complexation behavior of selected hydroxamic acids toward eight divalent ions, including Pd(II), Cd(II), Hg(II), Mn(II), Co(II), Ni(II), Cu(II), and Zn(II). All these metal ions are important constituents of metalloproteins and are also major pollutants of the environment,

and hence a scheme for their removal from the environment is essential. Several binding modes were considered in the work.

However, as very few theoretical studies on the complexation behavior of hydroxamic acids were available at that time, the authors (Kakkar et al. 2006a) first tested their methodology against the Cu(II) complexes of the three isomeric aminophenylhydroxamic acids, since their crystal data are available (Gaynor et al. 2001). They tested two LDA functionals and eight GGA functionals, employing numerical basis sets of double-ξ quality plus polarization functions (DNP) to describe the valence orbitals.

Although hydroxamate ions usually bind to metal ions through the two oxygen atoms (i.e., as (O,O)-bidentate chelating agents), other binding modes are also possible, and this range can be greatly increased if the hydroxamate ligand contains secondary binding groups, resulting in many diverse and intriguing structures (Milios et al. 2002). This was found in the complexes formed between the isomeric aminophenylhydroxamic acids ($AphaH_2$) and $CuSO_4{\cdot}5H_2O$ (Gaynor et al. 2001). While 4-aminophenylhydroxamic acid (4-$AphaH_2$) gives the simple square planar complex $Cu(4\text{-}AphaH)_2{\cdot}2H_2O$, 2-aminophenylhydroxamic acid (2-$AphaH_2$) gives a fused 'dimeric' metallocrown of the formula $[Cu_5(2\text{-}Apha)_4(\mu\text{-}SO_4){\cdot}(H_2O)_2]_2$, in which the metal ions display extensive magnetic coupling (with potential applications in the field of magnetoelectronics). The complex has a 'clam-like' structure, in which (2-$Apha^{2-}$) is doubly deprotonated 2-aminophenylhydroxamic acid. The coordination is through deprotonated nitrogen and it contains bridging hydroximate (−2) functions, combined with the $\{O,\mu_2\text{-}O'\}$ chelating/bridging mode. 3-aminophenylhydroxamic acid (3-$AphaH_2$) gives a trinuclear helical polymer of formula $[Cu_3(3\text{-}AphaH)_4SO_4{\cdot}(H_2O)]_n{\cdot}8H_2O$, which has a supramolecular structure with large open cavities, which can be useful in trapping guest molecules.

The ability to accurately describe the three structurally diverse complexes by different pseudopotentials was discussed by the authors (Kakkar et al. 2006a). The following conclusions were drawn: both the LDA geometries, particularly VWN, are in good agreement with experiment, but the gradient-corrected DFT methods tend to exaggerate the $Cu–O_1$ bond length when compared with the experimental (Gaynor et al. 2001) value. On the other hand, LDA-VWN overbinds the $Cu–O_4$ bond, yielding a bond length that is too short by 0.034 Å. Some of the GGA functionals, namely BOP, RPBE, and HCTH, are particularly bad when it comes to predicting Cu–O bond lengths. The only GGA functional that gives good agreement with experiment is PBE (Perdew et al. 1996), for which the error is only 1.6 % in relation to experiment, in spite of the fact that the latter refer to the solid state, which is subject to deformation because of solid state effects. In particular, this is the only method that produces equal $Cu–O_1$ and $Cu–O_2$ bond lengths (see Fig. 4) for the two rings, in agreement with experiment. All other methods predict asymmetry in the two rings. In most cases, the overall errors are smaller for bond angles than for bond distances.

The authors proceeded with the GGA-PBE method on the complexes. The 2-aminophenylhydroxamic acid isomer was found to be the most stable of the three, but the complexation energy values indicate slightly greater stability of

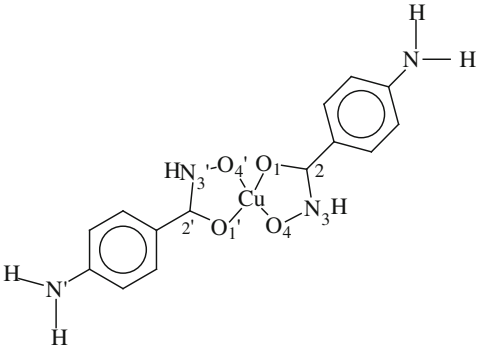

Fig. 4 Structure of the Cu(II) complex of 4-aminophenylhydroxamic acid

the 4-aminophenylhydroxamic acid complex. In each complex, both five-membered Cu-hydroxamate rings were found to be planar, causing delocalization of electrons in the $O_1C_2N_3$ moiety. The C_2C_6 bond is essentially single, permitting the phenyl ring to rotate about this bond. The phenyl rings are twisted with respect to the hydroxamate grouping by $\sim 20°$ in each case.

The group charge of the hydroxamate ligand changes from a value of -1.0 in the free state to ~ -0.3 in the three complexes, signifying electron transfer from the ligand to Cu(II) and coordination bond formation. The complexes were found to have sizable covalent character, each Cu–O bond having a covalent bond order slightly higher than 0.5.

Kakkar et al. (2006a) also observed that Mulliken charges are unreliable, as they are basis-size dependent. Plots of the electrostatic potential maps for the three complexes are shown in Fig. 5. These maps give an idea about the range of electron density around the complex. For 2- and 3-aminophenylhydroxamate complexes, the 0.016 au (10 kcal mol^{-1}) isoelectronic contour is plotted. However, for the 4-aminophenylhydroxamate complex, the potential extends only between -5.1×10^{-4} and 2.9×10^{-7} au, and hence the 1×10^{-10} au contour is plotted.

The three maps demonstrate the differences in the electronic behavior of the three complexes. The 2- and 3-aminophenylhydroxamate complexes exhibit similar contours. However, the map for the 4-aminophenylhydroxamate complex

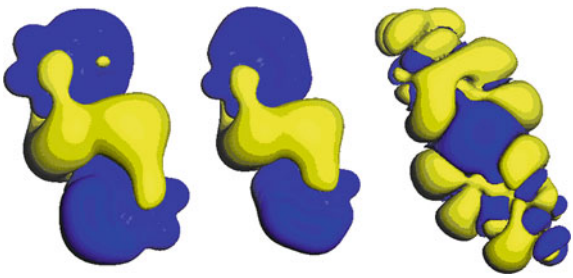

Fig. 5 Isopotential maps for the Cu(II) complex of 2- and 3-aminophenylhydroxamic acid (Isovalue = 0.016 au), and 4-aminophenylhydroxamic acid (Isovalue = 1×10^{-10} au)

bears no resemblance to that of the other two. The smaller extent of the potential in the case of the 4-aminophenylhydroxamate complex may explain its reluctance to polymerize.

4.3 Metal Ion Selectivity

Having shown that the GGA-PBE functional combined with the DZP basis set gives a satisfactory description of the bonding in the Cu(II) aminophenylhydroxamic acid complexes, Kakkar et al. (2006b) proceeded with DFT calculations on a number of square planar hydroxamate chelates of several divalent metal ions in order to determine their respective affinities for hydroxamic acid ligands. Except Mn(II), which prefers the quartet spin state, the metal ions were seen to prefer the low-spin state. Though the favored geometry is square planar, the Zn(II) complex is considerably distorted (Fig. 6).

The calculated binding mode (–NOH deprotonated) was found to be in agreement with experiment. The complexation energies follow the order Cd(II) < Mn(II) < Hg(II) < Zn(II) < Pd(II) < Co(II) < Cu(II) < Ni(II), which is almost the IW series, with two notable exceptions, Pd(II) and Ni(II), both of which are d^8 ions. The authors explained the lesser stability of Pd(II) complexes than that predicted from the IW series on the basis of the HSAB principle. The hydroxamate ligand contains negatively charged carboxylate-like oxygens, and is hence hard, and should not prefer the soft metal ions, Cd(II), Hg(II), and Pd(II). In fact, palladium shows a preference for the hydroximate binding mode (Hall et al. 2002). The other exception is Ni(II), for which the binding energy was found to be the largest. This was explained on the basis of higher covalent character in the Ni(II) complex.

Extensive calculations showed that, although the interactions are mainly dominated by electrostatic forces, there is a covalent contribution as well that introduces subtle variations in binding affinities of various metal ions. Thus, although a reasonable correlation was found between the complexation energies and reciprocals of the ionic radii of the metal ions, deviations were attributed to some covalent character of the metal–ligand bonds, which modify a ligand's affinity for a metal ion and introduce subtle variations that are ultimately responsible for their biological action. A linear relationship between the partial charge on the metal ion and the LUMO energy showed that metal ions with lower lying vacant orbitals are able to form covalent coordination with the FHA ligand. The covalent bond order of the metal–ligand bonds is quite high. The affinity of the formohydroxamate ion for Ni(II) is satisfactorily explained on the basis of larger charge transfer from the ligand, and is reflected in the Ni(II) ligand bond orders, which are close to unity. The authors (Kakkar et al. 2006b) discussed the bonding characteristics of the investigated complexes, as well as the optimum size of the metal binding site. Some other hydroxamic acids were also investigated in the

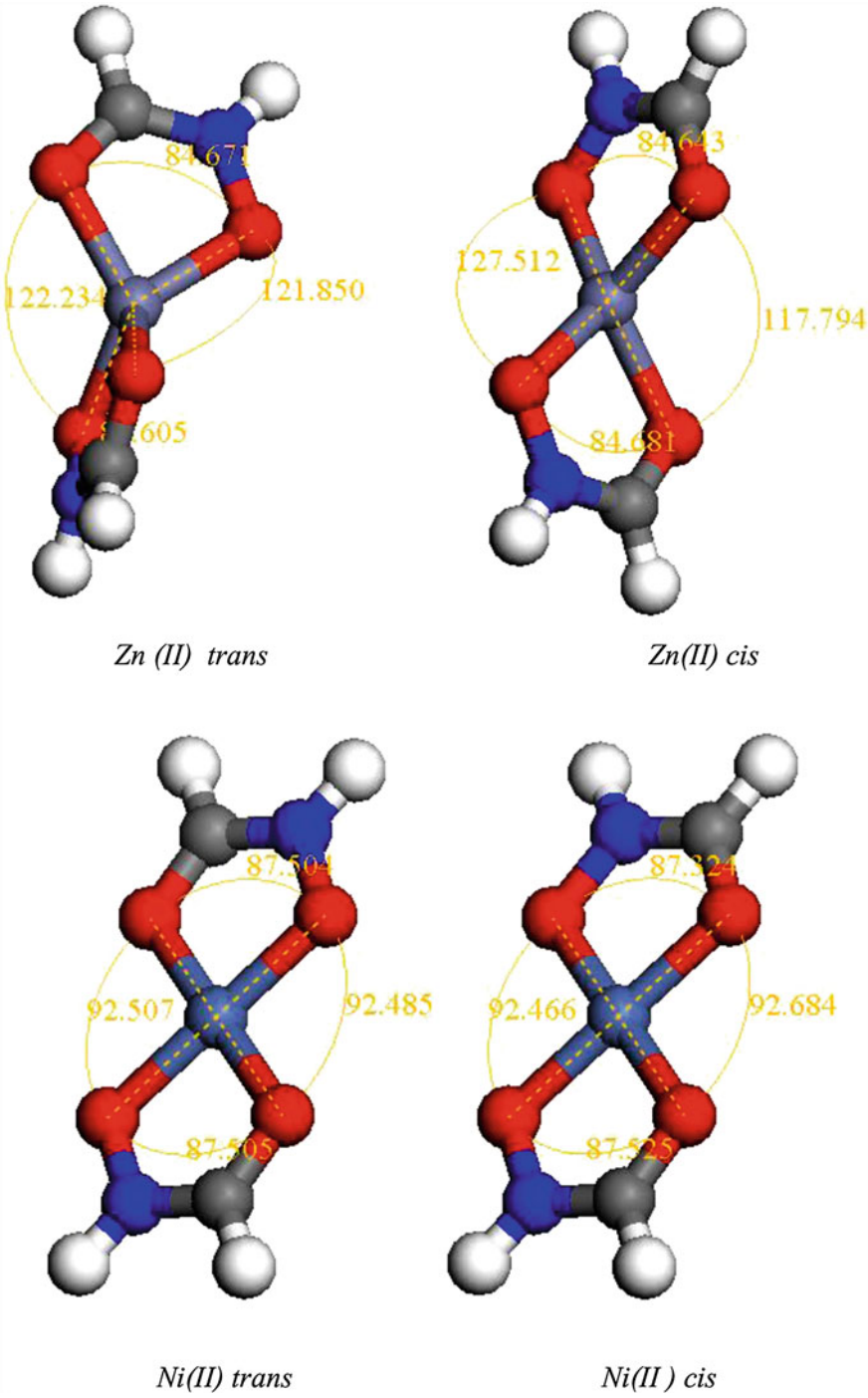

Fig. 6 Optimized structures of the *cis* and *trans* forms of the formohydroxamate complexes of Zn(II) and Ni(II). Color code: H-white, C-grey, N-blue, O-red. The top ring contains the M–O_2–C–N–O_1–(M = Zn, Ni) five-membered ring. The corresponding atoms of the lower ring are numbered with a prime

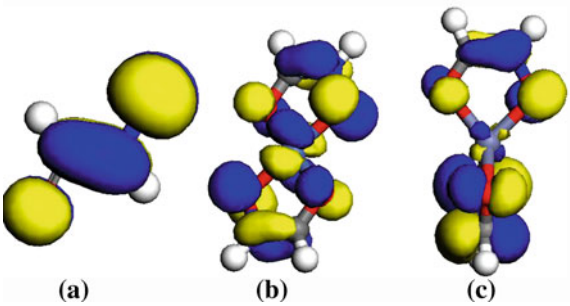

Fig. 7 Plot of the HOMOs for **a** formohydroxamate anion, and the *trans* formohydroxamate complexes of **b** Ni(II), and **c** Zn(II)

work. For hydroximate complexes and complexes with other hydroxamic acids, the Ni(II) complex was again found to be the most stable.

The plots of the highest occupied molecular orbitals of the ligand, the Ni(II) complex and the Zn(II) complex (Fig. 7) show that the ligand orbitals are retained in the HOMO of the complexes, but, in the case of Ni(II), the metal *d* orbital also becomes a part of the HOMO, showing an interaction between the Ni(II) *d* orbitals and the ligand. There is no participation of the metal orbitals for the Zn(II) complex.

The authors (Kakkar et al. 2006b) applied the knowledge gained about coordination bonding to investigate the metalloprotein urease and its inhibition by AHA.

5 Urease Inhibition

The interactions of transition metal ions with biomolecules (metalloproteins, peptides, DNA, RNA molecules, etc.) represent one of the fundamental aspects exploited by living organisms in performing their essential tasks. The role of transition metal ions in the structure and function of these systems is immense, though often unknown at the atomic or electronic level. One of the most important properties of bioinorganic systems is the relationship between molecular structure and energetics. Molecular structures can be efficiently studied by atomic resolution experimental techniques, but they do not provide any energy values. Thus, it is very tempting to complement bioinorganic experiments with energy evaluations, which can be presently achieved by state-of-the-art quantum mechanical calculations.

The metalloenzyme urease holds a very important place in the history of enzymology (Lippard 1995). Sumner (1926) crystallized the enzyme, but only some 50 years later was urease found to contain Ni(II) (Dixon et al. 1975) a transition metal previously recorded as an oddity with respect to biological activity. Urease catalyzes the hydrolysis of urea to ammonia and carbamate according to the equation

$$CO(NH_2)_2 + H_2O \rightarrow H_2NCOO^- + NH_4^+$$

in plants, algae, fungi, and several microorganisms (Ciurli et al. 1999). The carbamate produced simultaneously decomposes, at the physiological pH, to give a second molecule of ammonia and bicarbonate, according to the equation

$$H_2NCOO^- + H_2O \rightarrow HCO_3^- + NH_3$$

The hydrolysis of urea is difficult; the uncatalyzed reaction has never been observed (Blakeley et al. 1982). The stability of urea is attributed to its resonance energy (30–40 kcal mol^{-1}) (Wheland 1955). The enzyme converts urea into products at a rate 10^{14} times faster than the spontaneous decomposition rate (Blakeley et al. 1982).

Crystal structures of urease from three different microorganisms, *Klebsiella aerogenes* (KAU), *Bacillus pasteurii* (BPU), and *Helicobacter pylori* (HP), have been reported, providing a detailed picture of the active site (Jabri et al. 1995; Benini et al. 1999; Pearson et al. 2000; Ha et al. 2001). Hydroxamic acids are an important family of urease inhibitors. The most studied derivative is AHA, shown to behave as a slow-binding inhibitor (Dixon et al. 1975; Ciurli et al. 1999). The structure of the AHA-inhibited C319A mutant of KAU has been reported (Koga et al. 1998). The structure of the AHA-inhibited BPU has also been solved at 1.55 Å resolution (Benini et al. 2000). Manunza et al. (1999) performed MD calculations on the active site of urease from KAU and its adducts with urea, hydroxamic acid and N-(n-butyl)-phosphoric triamide (NBPT).

The quantum mechanical approach was used to model urease and its inhibition by AHA (Kakkar et al. 2006b) using the GGA-PBE DFT functional. For each of the ureases from two different microorganisms, KAU and HP, for which crystal structures have been determined (Jabri et al. 1995; Pearson et al. 2000; Ha et al. 2001), calculations were carried out for the uninhibited urease and its AHA inhibited structure. The urease from BPU has a similar structure to that from KAU, and was hence omitted from the analysis.

As the structures are too large for DFT calculations to be performed on the entire system, the active site consisting of the two nickel atoms and the ligands bound to them were modeled only, resulting in structures still having a formidable number of around 320 atoms.

5.1 Klebsiella Aerogenes Urease

The active site for in the native urease consists of two nickel atoms, complexed with *His* 133, *His* 135, *His* 245, *His* 271, KCX 216, *Asp* 359, and HOH 500–502. When complexed with AHA, the active site again consists of the two nickel atoms, *His* 133, *His* 135, *His* 245, *His* 271, KCX 216, and *Asp* 345, but HOH 500–502 are replaced by AHA, HAE 558, which bridges the two nickel atoms.

The final structures, labeled ***A*** (native) and ***E*** (complexed with AHA) are depicted in Fig. 8. In ***A***, it can be seen that one Ni(II) atom is complexed with KCX via Ox1, *His* 246 via ND1, HOH 500 and 501 via their oxygens and *His* 272 via NE2. Likewise, the second nickel atom is also pentacoordinate, being linked to *His* 134 and *His* 136 via NE2, KCX via Ox2, *Asp* via OD1, and HOH 500 and 502 via their oxygens. HOH 500 serves as a bridging group, and is present as the hydroxyl ion. The Ni…Ni distance is long (3.743 Å) because of the bridge. The overall charge on this fragment is +1.0.

In ***E***, on the other hand, one of the nickels (Ni(1)) is four coordinate. Hydroxamate is a bidendate ligand and binds to the two nickel atoms. Thus, Ni(2) coordinates to KCX via its oxygen Ox2, *His* 133, and *His* 135 via their nitrogens NE2, *Asp* 345 via OD1, and HAE via O1. Ni(1) is coordinated to *His* 245 via its nitrogen ND1, *His* 271 via its nitrogen NE2, KCX via Ox1, and HAE via O2. The overall charge on the fragment is +1.0. The Ni…Ni distance decreases slightly to 3.699 Å as a result of the hydroxamate bridging.

The electrophilic nature of the two nickels is obvious from the drastic decrease in positive charge from +2.0 each to $\sim$0.2. Contrary to expectations, the bridging OH group is positively charged and cannot behave as a nucleophile, as envisaged by most proposed reaction mechanisms for urease action. In fact, it is the free oxygen of the aspartate residue that has the maximum negative charge, and which probably behaves as a nucleophile to extract a proton from urea, causing it to decompose to ammonia and a bound cyanate (Barrios and Lippard 2000). Such a mechanism is in accord with the experimental observation of a rate of urea hydrolysis independent of pH, since this confirms that an internal atom is involved in the proton extraction. The electrostatic potential map for ***A***, shown in Fig. 9, also shows a negative potential only near the aspartate oxygen.

For the acetohydroxamate-complexed urease, too, there is a negative potential only near the aspartate oxygen (Fig. 9). This complex is further stabilized by hydrogen bonding between the aspartate oxygen and the NH proton of

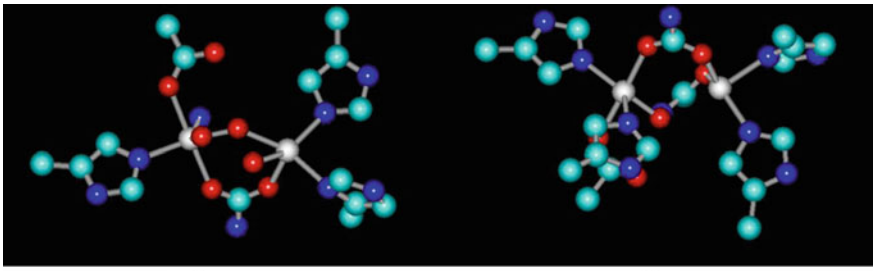

Fig. 8 Final structures of the native ***A*** and complexed with acetohydroxamic acid ***E*** taken for the study. Color code: carbons-cyan, nitrogens-blue, oxygens-red, nickels-white. Hydrogens have been omitted for clarity

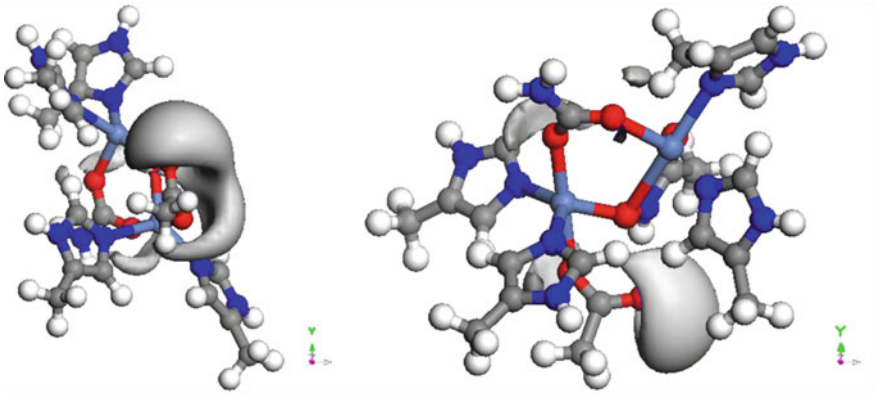

Fig. 9 Isopotential maps of ***A*** and ***E***

acetohydroxamate. Further, there is an overall slight positive charge (0.151) on the bound hydroxamate moiety. This is smaller than the positive charge on the OH moiety (0.538) it replaces, and is also reflected in an increase in the positive charge of the two nickels in the AHA-bound complex.

5.2 Helicobacter Pylori Urease

The active site for the native urease consists of two nickel atoms, complexed with *His* 136, *His* 138, *His* 248, *His* 274, KCX 219, *Asp* 362, and HOH 572. For the AHA-bound complex, the active site again consists of the two nickel atoms, *His* 136, *His* 138, *His* 248, *His* 274, KCX 219, and *Asp* 362, but HOH 572 is replaced by AHA, which bridges the two nickel atoms.

The final structures of ***Z*** (native) and ***Y*** (complexed with AHA) are depicted in Fig. 10. In ***Z***, it can be seen that one Ni(II) atom is complexed with KCX via Ox2,

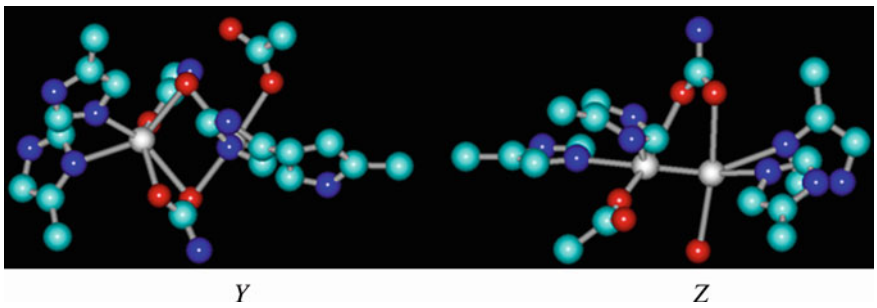

Fig. 10 Final structures of the ***Y*** and ***Z*** fragments taken for the study. Color code: carbons-cyan, nitrogens-blue, oxygens-red, nickel-white. Hydrogens have been omitted for clarity

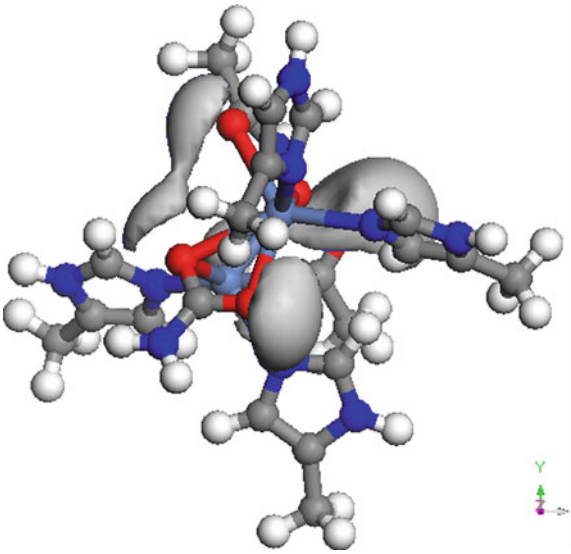

Fig. 11 Isopotential map of ***Y***

the other Ni, *His* 274 via NE2, water via its oxygen and *His* 248 via ND1. Likewise, the second nickel atom is also pentacoordinate, being linked to *His* 136 and *His* 138 via NE2, KCX via Ox2, *Asp* via OD1, and the other nickel atom. The overall charge on this moiety is +2. The Ni…Ni distance is short (2.128 Å). The overall charge on this fragment is +2.0.

In ***Y***, on the other hand, one of the nickels (Ni(2)) is hexacoordinate. Hydroxamate is a bidendate ligand and binds to the two nickel atoms. The octahedral coordination comes from the fact that in this case, there is coordination of this nickel atom with both the oxygens of KCX. Thus, Ni(2) coordinates to KCX via both oxygens Ox1 and Ox2, *His* 248 via ND1, *His* 274 via NE2, and HAE via O1 and O2. Ni(1) is coordinated to both *His* 136 and *His* 138 via their nitrogens NE2, KCX via its Ox2, *Asp* 362 via OD2, and HAE via O1. The overall charge on the fragment is +1.0. The Ni…Ni distance increases to 3.125 Å as a result of the hydroxamate bridging.

The nickels, especially Ni(1), in this case have higher positive charges ($\sim$0.5). The electrostatic potential map for ***Y***, shown in Fig. 11, also shows a negative potential only near the aspartate oxygen, although the negative charge on the aspartate oxygens is slightly smaller in this case.

6 Other Biological Applications

Hydroxamic acids exhibit a wide variety of biological activities (Kehl 1982). This has resulted in investigations on their role in biology, besides urease inhibition. Most of these studies have been directed at AHA. For instance, its interaction with

the vanadate ion has been studied both experimentally and theoretically (Duarte et al. 1998; Santos et al. 2003). Vanadate is a phosphate analog and can act as both an inhibitor of phosphate-metabolizing enzymes as well as an activator. It was found in these studies that AHA plays a role in the V(IV)/V(V) redox reaction.

Hydroxamic acids have also been investigated as siderophores (Santos et al. 1998; Edwards et al. 2005; Domagal-Goldman et al. 2009). In this connection, experimental and DFT studies have been performed (Edwards et al. 2005; Domagal-Goldman et al. 2009) on complexes of Fe(III) with desferrioxamine B (DFO-B), the most extensively studied siderophore with respect to mineral dissolution. DFO-B is a linear trihydroxamic acid composed of 1,5-diaminopentane and succinic acid residues.

Besides inhibition of urease, hydroxamic acids also inhibit a large number of other enzymes. Quantitative Structure Activity Relationship (QSAR) studies, MD, quantum mechanical, and docking studies directed toward the development of hydroxamic acid inhibitors for histone deacetylases (HDACs) (Dallavalle et al. 2009; Guo et al. 2005; Ragno et al. 2008), lipoxygenase (Hadjipavlou-Litina and Pontiki 2002), peptide deformylase (PDF) (Wang et al. 2006, 2008), MMPs (Hu and Shelver 2003; Kumar and Gupta 2003; Tuccinardi et al. 2006), and collagenase (Kumar and Gupta 2003) have been reported.

7 Conclusions

Hydroxamic acids find a number of applications in chemistry, biology, and geochemistry due to their roles as chelating agents, inhibitors of various enzymes, nitric oxide donors, siderophores, and many others. A large number of experimental and theoretical studies have been directed at understanding their unique chemistry. Theoretical studies have mostly focused on elucidation of the ground state structures and acidities. In particular, the smallest homolog, FHA, because of its small size, has been the subject of several theoretical studies ranging from semiempirical to high level ab initio and density functional. It is now well-established that this acid prefers the Z keto structure, in which there is strong intramolecular hydrogen bonding, and proton dissociation takes place from the nitrogen. It is also established that protonation of FHA occurs at the carbonyl oxygen. In solution, hydroxamic acids form intermolecular hydrogen bonds with the solvent, but the solvent is not able to dislodge the strong intramolecular hydrogen bonds. Hence, deprotonation from –OH is difficult, and this is reflected in the slower rate of complexion with metal ions.

It is heartening to note that the theoretical calculations complement experimental determinations. In fact, much of the literature concerns combined experimental and theoretical studies, and both are in accord with each other. This goes a long way in affirming belief in state-of-the-art theoretical calculations, which have now become possible, for small to medium-sized molecules, at least.

In spite of the fact that most of the applications of hydroxamic acids arise from their chelating abilities, very few theoretical studies have been reported, probably because of the difficulties in accurately modeling transition metal complexes. It is to be hoped that, with further increase in computational power and accurate basis sets for transition metals, we shall come close to completely deciphering metalloenzyme action. Some of the results obtained so far have shown that the hydroxamic acids are selective toward Ni(II) because of its electrophilicity and consequent covalent bond formation with the hydroxamate ligand, which uses the (O,O) coordination mode in its complexes. One of the most important applications of hydroxamic acids is as inhibitors of urease. Examination of the structures of urease from two organisms, KAU and HP, and their AHA complexes reveals that the Ni(II) ions are highly electrophilic and attract charge density from the bonded ligands. Most mechanisms hitherto proposed in the literature for urease action (Barrios and Lippard 2000) invoke a nucleophilic attack by the bridging OH on the electron deficient carbon of urea. Alternate mechanisms for urease action and inhibition (Milios et al. 2002) involve the extraction of a proton from the urea NH_2 group or the hydroxamic acid by the bridging hydroxyl. However, theoretical studies emphatically rule out the involvement of the bridging OH on two counts. The first is the positive charge on this group due to its proximity to two highly electrophilic Ni(II) ions and the other is the absence of this bridge in the urease from HP. Rather, the involvement of the oxygen of the aspartate ion, which is negatively charged, was proposed (Kakkar et al. 2006b). The formation of a hydrogen bond between the oxygen and the NH of AHA confirms its role in the binding. We feel that this examination of the urease active site should pave the way for the design of more efficient urease inhibitors.

References

Agrawal YK, Patel SA (1980) Hydroxamic acids: reagents for the solvent extraction and spectrophotometric determination of metals. Rev Anal Chem 4:237–238

Agrawal YK, Roshania RD (1980) Non-aqueous titrimetric determination of N-p-chlorophenylbenzohydroxamic acids: visual and potentiometric titration in dimethylformamide. Bull Soc Chim Belg 89:175–179

Al-Saadi AA (2012) Conformational analysis and vibrational assignments of benzohydroxamic acid and benzohydrazide. J Mol Struct 1023:115–122

Bagno A, Comuzzi C, Scorrano G (1994) Site of ionization of hydroxamic acids probed by heteronuclear NMR relaxation rate and NOE measurements. An experimental and theoretical study. J Am Chem Soc 116:916–924

Barocas A, Baroncelli F, Biondi GB, Grossi G (1966) The complexing power of hydroxamic acids and its effects on behaviour of organic extractants in the reprocessing of irradiated fuels II. J Inorg Nucl Chem 28:2961–2967

Baroncelli F, Grossi G (1965) The complexing power of hydroxamic acids and its effects on behaviour oforganic extractants in the reprocessing of irradiated fuels I. J Inorg Nucl Chem 27:1085–1092

Barrios AM, Lippard SJ (2000) Interaction of urea with a hydroxide-bridged dinuclear nickel center: an alternative model for the mechanism of urease. J Am Chem Soc 122:9172–9177

Bauer L, Exner O (1974) The chemistry of hydroxamic acids and *N*-hydroxyimides. Angew Chem Int Ed Engl 13:376–384

Benini S, Rypniewski WR, Wilson KS, Miletti S, Ciurli S, Mangani S (1999) A new proposal for urease mechanism based on the crystal structures of the native and inhibited enzyme from *Bacillus pasteurii*: why urea hydrolysis costs two nickels. Struct Fold Des 7:205–216

Benini S, Rypniewski WR, Wilson KS, Miletti S, Ciurli S, Mangani S (2000) The complex of *Bacillus pasteurii* urease with acetohydroxamate anion from X-ray data at 1.55 Å resolution. J Biol Inorg Chem 5:110–118

Bertini I, Briganti F, Scozzafava A (1995) In: Berthon G (ed) Handbook of metal–ligand interactions in biological fluids. Marcell-Dekker, New York, pp 81–91

Blakeley RL, Treston A, Andrews RK, Zerner B (1982) Nickel(II) promoted ethanolysis and hydrolysis N-(2-pyridylmethyl)urea. A model for urease. J Am Chem Soc 104:612–614

Blom CE, Günthard HH (1981) Rotational isomerism in methyl formate and methyl acetate; a low-temperature matrix infrared study using thermal molecular beams. Chem Phys Lett 84:267–271

Bordwell FG, Fried HE, Hughes DL, Lynch T-Y, Satish AV, Whang YE (1990) Acidities of carboxamides, hydroxamic acids, carbohydrazides, benzenesulfonamides, and benzenesulfonohydrazides in DMSO solution. J Org Chem 55:3330–3336

Bracher BH, Small RWH (1970) The crystal structure of acetohydroxamic acid hemihydrate. Acta Crystallogr B 26:1705–1709

Brown DA, Roche AL, Pakkanen TA, Pakkanen TT, Smolander K (1982) The X-ray crystal structure of bis(glycinohydroxamato)nickel(II). A novel co-ordination of nickel by a hydroxamic acid via the nitrogen atom of the NHOH group. J Chem Soc, Chem Commun 676–677

Brown DA, Glass WK, Mageswaran R, Ali Mohammed S (1991) ^{1}H and ^{13}C NMR studies of isomerism in hydroxamic acids. Magn Res Chem 29:40–45

Brown DA, Coogan RA, Fitzpatrick NJ, Glass WK, Abukshima DE, Shiels L, Ahlgrén M, Smolander K, Pakkanen TT, Pakkanen TA, Peräkylä M (1996) Conformational behaviour of hydroxamic acids: ab initio and structural studies. J Chem Soc, Perkin Trans 2:2673–2679

Brown DA, Cuffe L, Fitzpatrick NJ, Glass WK, Herlihy K (1998) COST D8 & ESF workshop on biological and medicinal aspects of metal speciation, JATE, Szeged, Hungary, 23–25 Aug 1998

Brown DA, Errington W, Glass WK, Haase W, Kemp TJ, Nimir H, Ostrovsky SM, Werner R (2001) Magnetic, spectroscopic, and structural studies of dicobalt hydroxamates and model hydrolases. Inorg Chem 40:5962–5971

Chittari P, Jadhav VR, Ganesh KN, Rajappa S (1998) Synthesis and metal complexation of chiral 3-mono-2-hydroxypyrrlopyrazine-1,4-diones or 3,3,-bis-allyl-2-hydroxy-pyrollopyrazine-1,4-diones. J Chem Soc, Perkin Trans I 1319–1324

Ciurli S, Benini S, Rypniewski WR, Wilson KS, Miletti S, Mangani S (1999) Structural properties of the nickel ions in urease: novel insights into the catalytic and inhibition mechanisms. Coord Chem Rev 190:331–355

Codd R (2008) Traversing the coordination chemistry and chemical biology of hydroxamic acids. Coord Chem Rev 252:1387–1408

Colston BJ, Choppin GR, Taylor RJ (2000) A preliminary study of the reduction of Np(VI) by formohydroxamic acid using stopped-flow near-infrared spectrophotometry. Radiochim Acta 88:329–334

Dallavalle S, Cincinelli R, Nannei R, Merlini L, Morini G, Penco S, Pisano C, Vesci L, Barbarino M, Zuco V, Cesare MD, Zunino F (2009) Design, synthesis, and evaluation of biphenyl-4-yl-acrylohydroxamic acid derivatives as histone deacetylase (HDAC) inhibitors. Eur J Med Chem 44:1900–1912

Decouzon M, Exner O, Gal J-F, Maria P-C (1990) The gas-phase acidity and the acidic site of acetohydroxamic acid: an FT-ICR study. J Org Chem 55:3980–3981

Denis P, Ventura ON (2001) Hydroxamic chelates of boric acid, a density functional study. J Mol Struct (Theochem) 537:173–180

Desaraju P, Winston A (1986) Synthesis and iron complexation studies of bis-hydroxamic acids. J Coord Chem 14:241–248

Dessi A, Micera G, Sanna D, Erre LS (1992) Vanadium(IV) and oxovanadium(IV) complexes of hydroxamic acids and related ligands. J Inorg Biochem 48:279–287

Dissanayake DP, Senthilnithy R (2009) Thermodynamic cycle for the calculation of ab initio pK_a values for hydroxamic acids. J Mol Struct (Theochem) 910:93–98

Dixon NE, Gazzola C, Watters JJ, Blakeley RL, Zerner B (1975) Jack bean urease (EC 3.5.1.5). A metalloenzyme. A simple biological role for nickel? J Am Chem Soc 97:4131–4133

Domagal-Goldman SD, Paul KW, Sparks DL, Kubicki JD (2009) Quantum chemical study of the Fe(III)-desferrioxamine B siderophore complex—electronic structure, vibrational frequencies, and equilibrium Fe-isotope fractionation. Geochim Cosmochim Acta 73:1–12

Duarte HA, Paniago EB, Carvalho S, De Almeida WB (1998) Interaction of N-hydroxyacetamide with vanadate: a density functional study. J Inorg Biochem 72:71–77

Edwards DC, Nielson SB, Jarzęcki AA, Spiro TG, Mynen SCB (2005) Experimental and theoretical vibrational spectroscopy studies of acetohydroxamic acid and desferrioxamine B in aqueous solution: effects of pH and iron complexation. Geochim Cosmochim Acta 69:3237–3248

Exner O (1964) Acyl derivatives of hydroxylamine. IX. A spectroscopic study of tautomerism of sulfohydroxamic acids. Collect Czech Chem Commun 29:1337–1343

Farkas E, Kozma E, Pethö M, Herlihy KM, Micera G (1998a) Equilibrium studies on copper(II)- and iron(III)-monohydroxamates. Polyhedron 17:3331–3342

Farkas E, Megyeri K, Somsák L, Kováks L (1998b) Interaction between Mo(VI) and siderophore models in aqueous solution. J Inorg Biochem 70:41–47

Farkas E, Enyedy ÉA, Micera G, Garribba E (2000) Coordination modes of hydroxamic acids in copper(II), nickel(II) and zinc(II) mixed-ligand complexes in aqueous solution. Polyhedron 19:1727–1736

Fishbein WN, Carbone PP (1965) Urease catalysis: II. Inhibition of the enzyme by hydroxyurea, hydroxylamine, and acetohydroxamic acid. J Biol Chem 240:2407–2414

Fitzpatrick NJ, Mageswaran R (1989) Theoretical study of hydroxamic acids. Polyhedron 8:2255–2263

García B, Ibeas S, Leal JM, Senent ML, Niño A, Muñoz-Caro C (2000) Theoretical and experimental study of the acetohydroxamic acid protonation: the solvent effect. Chem Eur J 6:2644–2652

García B, Ibeas S, Muñoz A, Leal JM, Ghinami C, Secco F, Venturini M (2003) NMR studies of phenylbenzohydroxamic acid and kinetics of complex formation with Nickel(II). Inorg Chem 42:5434–5441

García B, Ibeas S, Leal JM, Secco F, Venturini M, Senent ML, Niño A, Muñoz C (2005) Conformations, protonation sites, and metal complexation of benzohydroxamic acid. A theoretical and experimental study. Inorg Chem 44:2908–2919

García B, Secco F, Ibeas S, Muñoz A, Hoyuelos FJ, Leal JM, Senent ML, Venturini M (2007) Structural NMR and ab initio study of salicylhydroxamic and p-hydroxybenzohydroxamic acids: evidence for an extended aggregation. J Org Chem 72:7832–7840

Gaynor D, Starikova ZA, Haase W, Nolan KB (2001) Copper(II) complexes of isomeric aminophenylhydroxamic acids. A novel 'clam-like' dimeric metallacrown and polymeric helical structure containing interlinked unique copper(II) sites. J Chem Soc, Dalton Trans 1578–1581

Gece G, Bilgiç S (2010) A theoretical study of some hydroxamic acids as corrosion inhibitors for carbon steel. Corros Sci 52:3304–3308

Ghosh KK (1997) Kinetic and mechanistic aspects of acid catalysed hydrolysis of hydroxamic acids. Indian J Chem 36B:1089–1102

Guo J-X, Ho J-J (1999) Ab initio study of substitution effect and catalytic effect of intramolecular hydrogen transfer of N-substituted formamides. J Phys Chem A 103:6433–6441

Guo Y, Xiao J, Guo Z, Chu F, Cheng Y, Wu S (2005) Exploration of a binding mode of indole amide analogues as potent histone deacetylase inhibitors and 3D-QSAR analyses. Bioorg Med Chem 13:5424–5434

Ha N-C, Oh S-T, Sung JY, Cha KA, Lee MH, Oh B-H (2001) Supramolecular assembly and acid resistance of *Helicobacter pylori* urease. Nat Struct Biol 8:505–509

Hadjipavlou-Litina D, Pontiki E (2002) Quantitative–structure activity relationships on lipoxygenase inhibitors. IEJMD 1:134–141

Hashimoto S, Nakamura Y (1995) Nuclease activity of a hydroxamic acid derivative in the presence of various metal ions. J Chem Soc, Chem Commun 1413–1414

Hashimoto S, Nakamura Y (1996) Characterization of lanthanide-mediated DNA cleavage by intercalator-linked hydroxamic acids: comparison with transition systems. J Chem Soc, Perkin Trans 1 2623–2628

Hashimoto S, Ito S, Nakamura Y (1966) Nucleic acids sys series, vol 35. Oxford University Press, New York

Hashimoto S, Yamashita R, Nakamura Y (1992) DNA strand scissions by hydroxamic acids-copper(II) ion under aerobic conditions. Chem Lett 1639–1642

Hashimoto S, Itai K, Takeuchi Y, Nakamura Y (1997) Synthesis of bisnetropsin-linked hydroxamic acids and their DNA cleavage study in the presence of transition or lanthanide metal ions. Heterocyclic Commun 3:307–315

Hashimoto S, Yamamoto K, Yamada T, Nakamura Y (1998) Synthesis of bis(N-methylpyrrole oligopeptide-linked hydroxamic acids) and effective DNA cleavage by their vanadyl complexes. Heterocycles 48:939–947

Hall MD, Failes TW, Hibbs DE, Hambley TW (2002) Investigation of palladium(II) and platinum(II) complexes with salicylhydroxamic acid—structural and quantum mechanical studies. Inorg Chem 41:1223–1228

Hiriart MV, Corcuera LJ, Andrade C, Crivelli I (1985) Copper(II) complexes of a hydroxamic acid from maize. Phytochemistry 24:919–1922

Hu X, Shelver WH (2003) Docking studies of matrix metalloproteinase inhibitors: zinc parameter optimization to improve the binding free energy prediction. J Mol Graph Model 22:115–126

Jabri E, Carr MB, Hausinger RP, Karplus PA (1995) The crystal structure of urease from *Klebsiella aerogenes*. Science 268:998–1004

Jiang Y, Pan Y, Chen D, Wang F, Yan L, Li G, Xue Y (2012) A theoretical study of the effect of carboxyl hydroxamic acid on the flotation behaviour of diapore and aluminosilicate minerals. Clays Clay Miner 60:52–62

Joshi RR, Ganesh KN (1992) Chemical cleavage of plasmid DNA by Cu(II), Ni(II) and Co(III) desferal complexes. Biochem Biophys Res Commun 182:588–592

Joshi RR, Ganesh KN (1994a) Duplex and triplex directed DNA cleavage by oligonucleotide-Cu(II)/Co(II) metallodesferal conjugates. Biochim Biophys Acta 1201:454–460

Joshi RR, Ganesh KN (1994b) Metallodesferals as a new class of DNA cleavers: specificity, mechanism and targeting of DNA scission reactions. Proc-Indian Acad Sci, Chem Sci 106:1089–1108

Joshi KA, Gejji SP (2005) Electronic structure and vibrational analysis of AHA…HX complexes. Chem Phys Lett 415:110–114

Kaczor A, Proniewicz LM (2004) The structural study of acetohydroxamic and oxalodihydroxamic acids in DMSO solution based on the DFT calculations of NMR spectra. J Mol Struct 704:189–196

Kaczor A, Proniewicz LM (2005) Molecular structure of 2-(hydroxyimino)propanohydroxamic acid in solid state and DMSO solution. Spectrochim Acta, Part A 62:1023–1031

Kahn O (2000) Chemistry and physics of supramolecular materials. Acc Chem Res 33:647–657

Kakkar R, Grover R, Chadha P (2003) Conformational behavior of some hydroxamic acids. Org Biomol Chem 1:2200–2206

Kakkar R, Grover R, Gahlot P (2006a) Density functional study of the properties of isomeric aminophenylhydroxamic acids and their Cu(II) complexes. Polyhedron 25:759–766

Kakkar R, Grover R, Gahlot P (2006b) Metal ion selectivity of hydroxamates: a density functional study. J Mol Struct (Theochem) 767:175–184
Kaur D, Kohli R (2008) Intra and intermolecular hydrogen bonding in formohydroxamic acid. Int J Quantum Chem 108:119–134
Kaur D, Kohli R (2012) Understanding hydrogen bonding of hydroxamic acids with some amino acid side chain model molecules. Struct Chem 23:161–173
Kaur D, Kohli R, Kaur RP (2009) The role of isomerism and medium effects on stability of anions of formo and thioformohydroxamic acid. J Mol Struct (Theochem) 911:30–39
Kehl H (ed) (1982) Chemistry and biology of hydroxamic acids. Karger, New York
Koga T, Furutachi H, Nakamura T, Fukita N, Ohba M, Takahashi K, Okawa H (1998) Dinuclear nickel(II) complexes of phenol-based "end-off" compartmental ligands and their urea adducts relevant to the urease active site. Inorg Chem 37:989–996
Kumar D, Gupta SP (2003) A quantitative structure–activity relationship study on some matrix metalloproteinase and collagenase inhibitors. Bioorg Med Chem 11:421–426
Kurzak B, Kozlowski H, Farkas E (1992) Hydroxamic and amino hydroxamic acids and their complexes with metal ions. Coord Chem Rev 114:169–200
Larsen IK (1988) Structural characteristics of the hydroxamic acid group. Crystal structure of formohydroxamic acid. Acta Crystallogr B 44:527–533
Leung K (2006) Ab initio molecular dynamics study of the hydration of the formohydroxamate anion. Biophys Chem 124:222–228
Lindner HJ, Göttlicher S (1969) Die kristall- und molekülstruktur des eisen(III)-benzhydroxamat-trihydrates. Acta Crystallogr B 25:832–842
Lipczyñska-Kochany E, Iwamura H (1982) Oxygen-17 nuclear magnetic resonance studies. Pt. 10. Oxygen-17 nuclear magnetic resonance studies of the structures of benzohydroxamic acids and benzohydroxamate ions in solution. J Org Chem 47:5277–5282
Lippard SJ (1995) At last—the crystal structure of urease. Science 268:996–997
Lossen H (1869) Ueber die oxalohydroxamsäure. Justus Liebigs Ann Chem 150:314–320
Manunza B, Deiana S, Pintore M, Gessa C (1999) The binding mechanism of urea, hydroxamic acid and N-(N-butyl)-phosphoric triamide to the urease active site. A comparative molecular dynamics study. Soil Biol Biochem 31:789–796
Marmion CJ, Murphy T, Nolan KB, Docherty JR (2000) Hydroxamic acids are nitric oxide donors. Facile formation of ruthenium(II)-nitrosyls and NO-mediated activation of guanylate cyclase by hydroxamic acids. Chem Commun 13:1153–1154
Marmion CJ, Griffith D, Nolan KB (2004) Hydroxamic acids—an intriguing family of bioligands and enzyme inhibitors. Eur J Inorg Chem 15:3003–3016
Martin RB (1987) A stability ruler for metal ion complexes. J Chem Educ 64:402
McNaught AD, Wilkinson A (1997) IUPAC compendium of chemical terminology, 2nd edn (the "Gold Book"). Blackwell, Oxford
Milios CJ, Manessi-Zoupa E, Perlepes SP (2002) Modeling the coordination mode of hydroxamate inhibitors in urease: preparation, X-ray crystal structure and spectroscopic characterization of the dinuclear complex $[Ni_2(O_2CMe)(LH)_2(tmen)_2](O_2CMe)\cdot 0.9H_2O\cdot 0.6E$-tOH ($LH_2$ = benzohydroxamic acid; tmen = *N*,*N*,*N*′,*N*′-tetramethylethyleneamine). Trans Met Chem 27:864–873
Miller MJ (1989) Synthesis and therapeutic potential of hydroxamic base siderophores and analogues. Chem Rev 89:1563–1579, and references therein
Mora-Diez N, Senent ML, García B (2006) Ab initio study of solvent effects on the acetohydroxamic acid deprotonation processes. Chem Phys 324:350–358
Munoz-Caro C, Nino A, Senent ML, Leal JM, Ibeas S (2000) Modeling of protonation processes in acetohydroxamic acid. J Org Chem 65:405–410
Niño A, Muñoz-Caro C, Senent ML (2000) Suitability of different levels of theory for modelling of hydroxamic acids. J Mol Struct (Theochem) 530:291–300
Parr RG, Pearson RG (1983) Absolute hardness: companion parameter to absolute electronegativity. J Am Chem Soc 105:7512–7516
Pearson RG (1963) Hard and soft acids and bases. J Am Chem Soc 85:3533–3539

Pearson MA, Park I-S, Schaller RA, Michel LO, Karplus PA, Hausinger RP (2000) Kinetic and structural characterization of urease active site variants. Biochemistry 39:8575–8584

Perdew JP, Burke K, Ernzerhof M (1996) Generalized gradient approximation made simple. Phys Rev Lett 77:3865–3868

Ragno R, Simeoni S, Rotili D, Caroli A, Botta G, Brosch G, Massa S, Mai A (2008) Class II-selective histone deacetylase inhibitors. Part 2: alignment-independent GRIND 3-D QSAR, homology and docking studies. Eur J Med Chem 43:621–632

Raymond KN, Müller G, Matzanke BF (1984) Complexation of iron by siderophores a review of their solution and structural chemistry and biological function. Top Curr Chem 123:49–102

Remko M (2002) The gas-phase acidities of substituted hydroxamic and silahydroxamic acids: a comparative ab initio study. J Phys Chem A 20:5005–5010

Remko M, Šefčíková J (2000) Structure, reactivity and vibrational spectra of formohydroxamic and silaformohydroxamic acids: a comparative ab initio study. J Mol Struct (Theochem) 528:287–296

Remko M, Mach P, Schleyer PVR, Exner O (1993) Ab initio study of formohydroxamic acid isomers, their anions and protonated forms. J Mol Struct (Theochem) 279:139–150

Rulíšek L, Vondrášek J (1998) Coordination geometries of selected transition metal ions (Co^{2+}, Ni^{2+}, Cu^{2+}, Zn^{2+}, Cd^{2+}, and Hg^{2+}) in metalloproteins. J Inorg Biochem 71:115–127

Sałdyka M, Mielke Z (2002) Infrared matrix isolation studies and ab initio calculations of formhydroxamic acid. J Phys Chem A 106:3714–3721

Sałdyka M, Mielke Z (2003a) Cis-trans isomerism of the keto tautomer of formohydroxamic acid. Chem Phys Lett 371:713–718

Sałdyka M, Mielke Z (2003b) Photodecomposition of formohydroxamic acid. Matrix isolation FTIR and DFT studies. Phys Chem Chem Phys 5:4790–4797

Sałdyka M, Mielke Z (2004a) The interaction of formohydroxamic acid with nitrogen: FTIR matrix isolation and ab initio studies. J Mol Struct 708:183–188

Sałdyka M, Mielke Z (2004b) The interaction of formohydroxamic acid with carbon monoxide: FTIR matrix isolation and quantum chemistry studies. Chem Phys 300:209–216

Sałdyka M, Mielke Z (2005a) Intra- and intermolecular hydrogen bonding in formohydroxamic acid complexes with water and ammonia: infrared matrix isolation and theoretical study. Chem Phys 308:59–68

Sałdyka M, Mielke Z (2005b) Dimerization of the keto tautomer of acetohydroxamic acid—infrared matrix isolation and theoretical study. Spectrochim Acta, Part A 61:1491–1497

Sałdyka M, Mielke Z (2007) Keto–iminol tautomerism in acetohydroxamic and formohydroxamic acids. Vib Spectrosc 45:46–54

Sant'Anna CMR (2001) A semiempirical study on hydroxamic acids: formohydroxamic acid and derivatives of the allelochemical dimboa. Quim Nova 24:583–587

Santos MA, Gaspar M, Gonçalves MLSS, Amorim MT (1998) Siderophore analogues. A new bis-(amine, amide, hydroxamate) ligand. Synthesis, solution chemistry, electrochemistry and molecular mechanics calculations for the iron complex. Inorg Chim Acta 278:51–60

Santos JM, Carvalho S, Paniago EB, Duarte HA (2003) Potentiometric, spectrophotometric and density functional study of the interaction of *N*-hydroxyacetamide with oxovanadium(IV): the influence of ligand to the V(IV)/V(V) oxi-reduction reaction. J Inorg Biochem 95:14–24

Senent ML, Niño A, Muñoz Caro C, Ibeas S, García B, Leal JM, Secco F, Venturini M (2003) Deprotonation sites of acetohydroxamic acid isomers. A theoretical and experimental study. J Org Chem 68:6535–6542

Senthilkumar L, Kolandaivel P (2006) Molecular interaction study of formohydroxamic acid (FHA) with water. J Mol Struct 791:149–157

Senthilnithy R, Gunawardhana HD, De Costa MDP, Dissanayake DP (2006) Absolute pK_a determination for N-phenylbenzohydroxamic acid derivatives. J Mol Struct (Theochem) 761:21–26

Senthilnithy R, Weerasinghe S, Dissanayake DP (2008) Stability of hydroxamate ions in aqueous medium. J Mol Struct (Theochem) 851:109–114

Sigel H, McCormick DB (1970) On the discriminating behavior of metal ions and ligands with regard to their biological significance. Acc Chem Res 3:201–208

Šille J, Garaj V, Ježko P, Remko M (2010) Gas phase and solution stability of complexes L…M, where M = Li^+, Na^+, K^+, Mg^{2+}, or Ca^{2+} and L = R-(CO)NHOH (R = H, NH_2, CH_3, CF_3, or phenyl). Acta Facultatis Pharmaceuticae Universitatis Comenianae Tomus L VII:1–18

Sumner JB (1926) The isolation and crystallization of the enzyme urease: preliminary paper. J Biol Chem 69:435–441

Tavakol H (2009) Computational study of simple and water-assisted tautomerism of hydroxamic acids. J Mol Struct (Theochem) 916:172–179

Taylor RJ, May I, Wallwork AL, Dennis IS, Hill NJ, Galkin BY, Zilberman BY, Fedorov YS (1998) The applications of formo- and aceto-hydroxamic acids in nuclear fuel reprocessing. J Alloy Compd 271–273:534–537

Tipton CL, Buell EL (1970) Ferric iron complexes of hydroxamic acids. Phytochemistry 9:1215–1217

Todd TA, Wigelund RA (2006) Advanced separation technologies for processing spent nuclear fuel and the potential benefits to a geologic repository. In: Lumetta GJ, Nash KL, Clark SB, Friese JI (eds) Separations for the nuclear fuel cycle in the 21st century. ACS symposium series, vol 933. ACS, Washington, pp 41–56

Tuccinardi T, Martinelli A, Nuti E, Carelli P, Balzano F, Uccello-Barretta G, Murphy G, Rossello A (2006) Amber force field implementation, molecular modelling study, synthesis and MMP-1/MMP-2 inhibition profile of (R)-and (S)-N-hydroxy-2-(N-isopropoxybiphenyl-4-ylsulfonamido)-3-methylbutanamides. Bioorg Med Chem 14:4260–4276

Turi L, Dannenberg JJ, Rama J, Ventura ON (1992) Molecular orbital study of the structures of hydroxamic acids. J Phys Chem 96:3709–3712

Ventura ON, Rama JB, Turi L, Dannenberg JJ (1993) Acidity of hydroxamic acids: an ab initio and semiempirical study. J Am Chem Soc 115:5754–5761

Vrcek IV, Kos I, Weitner T, Birus M (2008) Acido-base behavior of hydroxamic acids: experimental and ab initio studies on hydroxyureas. J Phys Chem A 112:11756–11768

Wang X, Houk KN (1988) Theoretical elucidation of the origin of the anomalously high acidity of Meldrum's acid. J Am Chem Soc 110:1870–1872

Wang Q, Zhang D, Wang J, Cai Z, Xu W (2006) Docking studies of nickel-peptide deformylase (PDF) inhibitors: exploring the new binding pockets. Biophys Chem 122:43–49

Wang Q, Wang J, Cai Z, Xu W (2008) Prediction of the binding modes between BB-83698 and peptide deformylase from Bacillus stearothermophilus by docking and molecular dynamics simulation. Biophys Chem 134:178–184

Weinberg ED (1989) Quart Rev Biol 64:261–290

Wheland GW (1955) Resonance in organic chemistry. Wiley, New York

Wiberg KB, Laidig KE (1988) Acidity of (Z)- and (E)-methyl acetates: relationship to Meldrum's acid. J Am Chem Soc 110:1872–1874

Wu D-H, Ho J-J (1998) Ab initio study of intramolecular proton transfer in formohydroxamic acid. J Phys Chem A 102:3582–3586

Yamin LJ, Ponce CA, Estrada MR, Vert FT (1996) Protonation and deprotonation of hydroxamic acids. An MO ab initio study. J Mol Struct (Theochem) 360:109–117

Yazal JE, Pang Y-P (1999) Novel stable configurations and tautomers of the neutral and deprotonated hydroxamic acids predicted from high-level ab initio calculations. J Phys Chem A 103:8346–8350

Yen S-J, Lin C-Y, Ho J-J (2000) Ab initio study of proton transfer between protonated formohydroxamic acid and water molecules. J Phys Chem A 104:11771–11776

http://www.springer.com/978-3-642-38110-2

Hydroxamic Acids
A Unique Family of Chemicals with Multiple Biological Activities
Gupta, S.P. (Ed.)
2013, X, 312 p. 366 illus., 27 illus. in color., Hardcover
ISBN: 978-3-642-38110-2